206182

NASA GRANT NAG-1-1876

A NEW APPROACH FOR DETERMINING ONSET OF TRANSITION

FINAL REPORT

Prepared by

H. A. Hassan

Department of Mechanical and Aerospace Engineering
Post Office Box 7910
North Carolina State University
Raleigh, North Carolina 27695-7910

ABSTRACT

The final report consists of three papers[1-3] published under this grant. These papers outline and demonstrate the new method for determining transition onset. The procedure developed under this grant requires specification of the instability mechanism, i.e., Tollmien-Schlichting or crossflow, that leads to transition.

1. Warren, E. S. and Hassan, H. A., "An Alternative to the e^n Method for Determining Onset of Transition," AIAA Paper 97-0825, January 1997.
2. Warren, E. S. and Hassan, H. A., "A Transition Model for Swept Wing Flows," AIAA Paper 97-2245, June 1997.
3. Warren, E. S. and Hassan, H. A., "A Transition Closure Model for Predicting Transition Onset," SAE Paper 975502, October 1997.

AIAA 97-0825
An Alternative to the e^n Method for Determining Onset of Transition

E. S. Warren and H. A. Hassan
North Carolina State University
Raleigh, NC

35th Aerospace Sciences Meeting & Exhibit

January 6-10,1997 / Reno, NV

An Alternative to the e^n Method for Determining Onset of Transition

E. S. Warren* and H. A. Hassan†
North Carolina State University, Raleigh, NC 27695-7910

Abstract

A new approach has been developed to determine the onset of transition. The approach is based on a two-equation model similar to those used in the study of turbulence. The approach incorporates information from linear stability theory on streamwise or Tollmien-Schlichting instabilities. The present approach has proven to be an inexpensive alternative to the e^n method for determining the onset of transition on a flat plate and airfoil for a variety of Reynolds numbers and freestream intensities. Further, the method is incorporated into two flow solvers, boundary layer and Navier-Stokes. This made it possible to calculate the laminar, transitional, and turbulent regions in a single computation.

Introduction

The process of transition from laminar to turbulent flow remains one of the most important unsolved problems in fluid mechanics and aerodynamics. Virtually all flows of engineering interest transition from laminar to turbulent flow. Because transitional flows are characterized by increased skin friction and heat transfer, the accurate determination of heating rates and drag critically depend upon the ability to predict the onset and extent of transition. However, no mathematical model exists which can accurately predict the location of transition under a wide range of conditions. Design engineers resort to methods which are based on either empirical correlations or linear stability theory.

The e^n method is currently the method of choice for determining transition onset. The method is based on linear stability theory and generally requires the following steps

(i) Pre-calculation of mean flow at a large number of streamwise locations along the body of interest.

(ii) At each streamwise station, a local linear stability analysis is performed. By assumptions of the linear theory, the unsteady disturbances are decomposed into separate normal modes of different frequency. The stability equations are solved for the spatial amplification rate of each unstable frequency.

(iii) An amplitude ratio for each frequency is then calculated by integrating the spatial amplification rate in the streamwise direction on the body, i.e.

$$\ln\left(\frac{A}{A_o}\right) = \int_{x_o}^{x} \alpha_i \, dx \qquad (1)$$

(iv) The n factor is then determined by taking the maximum of the above quantity at each streamwise location.

The major problem with the e^n method is that the n factor does not represent the amplitude of a disturbance in the boundary layer but rather an amplification *factor* from an unknown amplitude A_o. The amplitude A_o represents the amplitude of a disturbance of specified frequency at its neutral stability point. Its value is related to the external disturbance environment through some generally unknown receptivity process. As a consequence, the value of n which determines transition onset must be correlated to available experimental data. Unfortunately, the method suffers from the fact that n is not constant; moreover, the method is not useful in predicting transition onset on three dimensional configurations especially when the crossflow instability is important.[1, 2] Additionally, the e^n method requires the use of several computational tools such as

*Research Assistant, Mechanical and Aerospace Engineering, Student Member AIAA.
†Professor, Mechanical and Aerospace Engineering, Associate Fellow AIAA.

a boundary layer or Navier-Stokes flow solver to calculate the mean flow and the linear stability solver to determine the amplification rates. The process requires significant input from the designer and generally requires substantial knowledge of linear stability concepts. Methods based on the parabolized stability equations[3] (PSE) are being used to determine transition onset but they have not received the wide acceptance enjoyed by the e^n method. Methods based on the PSE also require pre-calculation of the mean flow and specification of initial conditions such as frequency and disturbance eigenfunctions. Methods based on linear stability theory only provide an estimation of the location of transition and can provide no information about the subsequent turbulent flow.

In this work, a different approach has been developed which does not require pre-calculation of the mean flow and includes the laminar, transitional, and turbulent regions in a single computation. The approach employs a two-equation model similar to that employed in turbulent calculations. It is based on the premise that, if a flow quantity can be written as the sum of a mean and a fluctuating quantity, then the *exact* equations that govern the fluctuations and their averages are identical irrespective of the nature of the oscillations, i.e., laminar, transitional or turbulent. Moreover, if it is possible to model the equations governing the mean energy of the fluctuations and their rate of decay (or other equations) in such a way that one does not appeal to their nature, then the resulting model equations will be formally identical. However, the parameters that appear in the modeled equations will depend on the nature of the fluctuations. As an illustration, let us assume that we employ a Boussinesq approximation to model the stresses resulting from the fluctuations, i.e.

$$\tau_{ij} = -\overline{\rho u_i' u_j'} = \mu_t \left(2\, S_{ij} - \frac{2}{3}\delta_{ij}\frac{\partial U_m}{\partial x_m} \right) - \frac{2}{3}\rho k \delta_{ij} \quad (2)$$

where

$$S_{ij} = \frac{1}{2}\left[\frac{\partial U_i}{\partial x_j} + \frac{\partial U_j}{\partial x_i} \right]$$

$$k = \frac{1}{2}\overline{u_i' u_i'}$$

ρ is the density, U_i is the mean velocity, δ_{ij} is the Kronecker delta and μ_t is the coefficient of viscosity brought about by the presence of fluctuations. The form indicated in Eq. (2) is used for both laminar and turbulence fluctuations but the expressions for μ_t are quite different because the physics governing them is different.

The goal stated above has recently been accomplished.[4] In that work, a new turbulence model was developed based on the exact equations governing the variance of velocity (kinetic energy) and the variance of vorticity (enstrophy). The form of the resulting equations was arrived at *without* making use of the fact that the flow was turbulent. Therefore, the modeled equations apply to flows of any nature, whether laminar, transitional or turbulent. In order to apply the modeled equations it is necessary to specify a "stress-strain relation." In Ref. [4] the set of equations was applied to turbulent flows. This allowed the model constants to be determined by comparing with experimental data.

The approach followed in this investigation is based on the modeled equations of Ref. [4] but with different "stress-strain relations." Further, it is assumed that the model constants derived in Ref. [4] remain unchanged.

To show the nature of the new "stress-strain relations," Eqs. (25) and (27) of Ref. [4] are re-written as

$$\frac{Dk}{Dt} = -\overline{u_i' u_j'}\frac{\partial U_i}{\partial x_j} - \frac{k}{\tau_k} + \frac{\partial}{\partial x_j}\left[\left(\frac{\nu}{3} + \frac{\nu_t}{\sigma_k} \right) \frac{\partial k}{\partial x_j} \right] \quad (3)$$

$$\begin{aligned} \frac{D\zeta}{Dt} &= -\frac{\partial \Omega_i}{\partial x_j}\left(\frac{1}{\sigma_r}\left[\frac{\partial(\nu_t \Omega_i)}{\partial x_j} + \frac{(\partial \nu_t \Omega_j)}{\partial x_i} \right] \right. \\ &\quad \left. + \frac{\epsilon_{mij}}{2}\left[\frac{\partial\left(\overline{u_m' u_l'}\right)}{\partial x_l} - \frac{\partial k}{\partial x_m} \right] \right) \\ &\quad + \frac{\partial}{\partial x_j}\left[\left(\nu + \frac{\nu_t}{\sigma_\zeta} \right) \frac{\partial \zeta}{\partial x_j} \right] - \frac{\beta_5}{R_k + \delta}\zeta^{\frac{3}{2}} \\ &\quad + \left(\alpha_3 \zeta b_{ij} + \frac{1}{3}\delta_{ij}\zeta \right) S_{ij} - \frac{\zeta \tau_{ij} \Omega_i \Omega_j \beta_4}{\rho k \Omega} \\ &\quad + 2\epsilon_{ilm}\beta_8 \left(\frac{\tau_{ij}}{\rho k} \right) \left(\frac{\partial k}{\partial x_l}\frac{\partial \zeta}{\partial x_m} \right) \frac{\Omega_j}{S^2} \\ &\quad - \frac{2\beta_6 \tau_{ij} \nu_t}{\rho k \nu} \Omega \Omega_i \Omega_j + \frac{\beta_7 \zeta}{\Omega^2} \Omega_i \Omega_j S_{ij} \end{aligned} \quad (4)$$

where

$$R_k = \frac{k}{\nu\sqrt{\zeta}}, \quad \nu_t = \frac{\mu_t}{\rho}, \quad S = \sqrt{S_{ij}S_{ij}}, \quad \Omega = \sqrt{\Omega_i \Omega_i}$$

$$R_T = \frac{k^2}{\nu\zeta}, \quad \zeta = \overline{\omega_i' \omega_i'}, \quad \omega_i' = \epsilon_{ilm}\partial_l u_m', \quad \Omega_i = \epsilon_{ilm}\partial_l U_m$$

and,

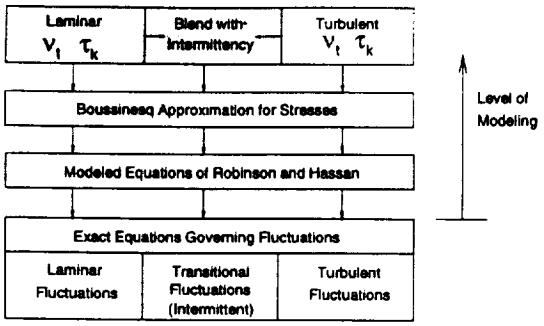

Figure 1: Schematic of modeling objectives in present work

$$f_{\mu_t} = \min(f^*_{\mu_t}, 1) \tag{5}$$

$$f^*_{\mu_t} = \left(1 + \frac{C_{\mu_1}}{R_T^{\frac{3}{2}}}\right)\left[1 - \exp\left(\frac{-\sqrt{k}y}{\nu C_{\mu_2}}\right)\right] \tag{6}$$

τ_k is a representative decay time for the kinetic energy and ν_t is the kinematic eddy viscosity. The closure coefficients for the model are given in Table 1.

As may be seen from the governing equations, one needs to specify ν_t and τ_k to effect closure. Within the laminar region, these quantities will be determined based on results of linear stability theory. The shaded areas of Figure 1 illustrate the objectives of the current approach. The diagram shows that the exact equations govern the fluctuations regardless of their nature, i.e. laminar, transitional, or turbulent. The stresses are then modeled by the Boussinesq approximation for all types of fluctuations. The work of Robinson and Hassan[5] developed expressions for ν_t and τ_k in the turbulent region. The current work develops expressions for ν_t and τ_k in the laminar and transitional regions.

For subsonic Mach numbers and regions where crossflow instability is unimportant, the dominant mode of instability is the first mode or the Tollmien-Schlichting (T-S) mode. For low speed flows, the dominant disturbance frequency at breakdown is well predicted by the frequency of the first mode disturbance having the maximum amplification rate. Using the work of Obremski et al.,[6] Walker[7] showed that this frequency can be correlated by

$$\frac{\omega\nu}{U_e^2} = 3.2 Re_{\delta^*}^{-3/2} \tag{7}$$

where U_e is the velocity at the edge of the boundary layer, Re_{δ^*} is the edge Reynolds number based on displacement thickness δ^*, and ω is the frequency.

The eddy viscosity resulting from fluctuations in the laminar region can be modeled by

$$\nu_t = C_\mu \, k \, \tau_{\mu_\ell}, \quad C_\mu = 0.09 \tag{8}$$

where τ_{μ_ℓ} is a viscosity time scale. Using the frequency of the dominant T-S disturbance, the viscosity time scale can be modeled in the laminar region as

$$\tau_{\mu_\ell} = \frac{a}{\omega} \tag{9}$$

where a is a model constant. Within the laminar region, the representative decay time for the kinetic energy is modeled as

$$\frac{1}{\tau_{k_\ell}} = a \frac{\nu_t}{\nu} S \tag{10}$$

Following the work of Robinson and Hassan[5], the turbulent region time scales are given as

$$\tau_{\mu_t} = \frac{k}{\nu\zeta} f_{\mu_t} \tag{11}$$

and

$$\frac{1}{\tau_{k_t}} = \frac{\nu\zeta}{k} \tag{12}$$

The two regions can be combined by using the concept of the intermittency. The intermittency, Γ represents the fraction of time that the flow is turbulent. At a given point, the flow is laminar $(1-\Gamma)$ of the time and turbulent Γ of the time. This allows the viscosity time scale to be written as a *transitional* viscosity time scale, i.e.

$$\tau_\mu = (1-\Gamma)\tau_{\mu_\ell} + \Gamma\tau_{\mu_t} \tag{13}$$

Combining Eqs. 8, 9, and 11 a *transitional* eddy viscosity can be written as

$$\nu_t = C_\mu \, f_\mu \, k \, \tau_\mu \tag{14}$$

where

$$\tau_\mu = (1-\Gamma)\left(\frac{a}{\omega}\right) + \Gamma\left(\frac{k}{\nu\zeta}\right) \tag{15}$$

and

$$f_\mu = 1 + \Gamma(f_{\mu_t} - 1) \tag{16}$$

Following a similar approach, the transitional decay time for the kinetic energy can be written

$$\frac{1}{\tau_k} = (1-\Gamma)\left(a\frac{\nu_t}{\nu}S\right) + \Gamma\left(\frac{\nu\zeta}{k}\right) \qquad (17)$$

The intermittency, Γ, is currently given by the Narasimha et al.[8] expression

$$\Gamma(x) = 1 - \exp\left(-A\xi^2\right) \qquad (18)$$

with

$$\xi = \max(x - x_t, 0)/\lambda, \quad A = 0.412 \qquad (19)$$

where x_t denotes the transition point and λ characterizes the extent of transition. For attached flows, an experimental correlation between λ and x_t is

$$Re_\lambda = 9.0 Re_{x_t}^{0.75} \qquad (20)$$

The transition point x_t is determined as a part of the solution procedure and will be discussed along with the results.

Results and Discussion

I. Implementation in Boundary Layer Solver

The present model was initially incorporated into the boundary layer code of Harris et al.[9] For such a calculation, initial profiles are needed to begin the marching procedure. For an initial station s along the surface, the dominant disturbance frequency is given by Eq. 7. This frequency was then employed in the linear stability code of Macaraeg et al.[10] to calculate the eigenvalues and eigenfunctions which make up the velocity disturbance. The velocity disturbance corresponding to this dominant frequency can written as

$$u_i' = u_i(y)\exp\left[i(\alpha s - \omega t)\right] + \text{c.c.} \qquad (21)$$

where α, the complex spatial amplification rate, and $u_i(y)$, the eigenfunction, are determined from the stability code for the specified frequency. The initial profile of k is then calculated from

$$k = \frac{1}{2}\overline{u_i' u_i'} \qquad (22)$$

The amplitude of the disturbance was set from the specified freestream intensity Tu defined as

$$Tu = 100\sqrt{\frac{2}{3}\frac{k_\infty}{U_\infty^2}} \qquad (23)$$

Note that in the laminar region, Eq. 3 does not depend on ζ. An initial profile for ζ is needed for the marching procedure but results were found to be independent of the choice of the ζ profile.

The model constant a is determined in the current work by comparing with the flat-plate experiments of Schubauer and Klebanoff[11] and Schubauer and Skramstad.[12] These classical experiments are well documented in the literature and cover a range of freestream turbulence intensities. The constant is correlated as a function of the freestream intensity as

$$a = 0.0095 - 0.019\,Tu + 0.069(Tu)^2 \qquad (24)$$

Figures 2 and 3 show the effect of the initial profiles on the onset of transition by plotting skin friction as a function of position along the plate. X_o is the location where the solution was started and X_t is the location of minimum skin friction. Figure 2 compares the present approach with the experiment of Ref.[11], while Figure 3 compares with the $Tu = 0.2$ experiment of Ref.[12]. Both figures clearly illustrate that the calculated X_t values are almost independent of X_o and are well within the scatter of the experimental results.

The rms amplitude ratio of the velocity disturbance can be obtained from the kinetic energy of the fluctuations as

$$A = \sqrt{k} = \sqrt{\frac{\overline{u'^2} + \overline{v'^2} + \overline{w'^2}}{2}} \qquad (25)$$

For the natural transition process there is a region of linear growth, followed by a region of non-linear growth which occurs as the amplitude of the velocity disturbance becomes sufficiently large. Transition occurs after the onset of the non-linear growth and this non-linear growth continues through the transitional region. After the non-linear growth region the modes which make up the disturbance become saturated. This saturation of modes characterizes the turbulent region. Figure 4 is a plot of the amplitude ratio as calculated by the present method for laminar flow (i.e. $\Gamma = 0$), with k_o representing the initial amplitude of k. As can be seen from the figure, the present method does predict the expected linear, non-linear, and saturated regions.

The location of minimum skin friction is commonly taken as the onset of transition. In practice, it is very difficult to determine the minimum skin friction point in an evolving calculation. This can be due to either the transient nature of Navier-Stokes calculations or due to local oscillations in the skin friction itself as seen in later airfoil results. To

alleviate this problem, an alternate criteria was developed by comparing with the flat plate results. It was observed that the present method predicted the local skin friction minimum at a location along the plate where the maximum $\frac{\nu_t}{\nu} \approx 9\%$. This criteria can be stated differently by noting that the "turbulent" Reynolds number, R_T, can be written in the laminar region ($\Gamma = 0$) as

$$R_T = \frac{1}{C_\mu} \frac{\nu_t}{\nu} \tag{26}$$

Written in this form, R_T can be considered a fluctuation Reynolds number instead of a turbulent Reynolds number. The location of transition onset, x_t, is then determined as the minimum distance along the surface for which $R_T \geq 1$.

Using this criteria Figure 5 compares the results for the present method with the skin friction experimental data of Ref.[11]. As seen from the figure, the present method does a good job of predicting the transition onset as well as the transitional and turbulent regions. Results for the present method are summarized in Table 2. As seen from the data, the onset of transition predicted by the current method compares well with the experimentally observed locations.

To determine the validity of the correlation for the model constant, a, the airfoil experiments of Mateer et al.[13] were considered. The two-dimensional airfoil shown in Figure 6 was used in the experiments over a range of angle of attack and Reynolds number. The angle of attack considered was $-0.5°$ at Reynolds numbers of 0.6, 2, and 6 million. The Mach number was 0.2 and the freestream rms pressure and velocity fluctuation levels were $0.02q_\infty$ and $0.005U_\infty$ respectively.

Figures 7 through 9 compare the skin friction results for the airfoil with the experimental data and Navier-Stokes predictions of Ref. [13]. The Navier-Stokes results of Ref. [13] were obtained using the e^n method and the turbulence model of Menter.[14] The boundary layer results for the present method were computed by using the boundary layer code of Harris et al.[9] with a pressure distribution obtained from an Euler solver. The initial profile of k for these airfoil cases was chosen as the freestream value.

Figure 7 compares the results of the present method for the $Re_c = 6x10^6$ case. Better agreement with the experimental data is seen with the transition onset prediction of the current method when compared with the prediction of the e^n method. For the airfoil results presented, the e^n method did not predict transition for the upper surface at all. Transition for the e^n method was determined on the upper surface by the location where the laminar boundary layer began to separate. Figure 8 presents the results for the $Re_c = 2x10^6$ case. Again, the present method does a better job of predicting transition onset. Figure 9 presents the results for the $Re_c = 0.6x10^6$ case. As seen from the data and discussed in Ref. [13], the boundary layer is very close to separation. Computations with the boundary layer code are not able to continue past the separation point.

II. Implementation in Navier-Stokes Solver

The present method has also been incorporated in a Navier-Stokes solver. This eliminates the need for obtaining the pressure distribution required by boundary layer type methods. Additionally, since the Navier-Stokes approach is a time marching scheme instead of a spatial marching scheme, specifying initial spatial profiles of k and ζ is not possible. By using the Navier-Stokes approach, the need for linear stability theory to provide an initial profile is eliminated. Additionally, it is no longer necessary to specify a pressure distribution.

Figure 5 again compares the results for the present method with the skin friction experimental data of Ref.[11]. As seen from the figure, the Navier-Stokes and boundary layer approaches predict the same transition onset location but the Navier-Stokes approach predicts a slightly higher value of the skin friction in the transition region.

Figures 7 through 9 also compare the skin friction calculated by the present method with the Navier-Stokes approach with experiment and other computations. Figure 7 compares the results for the $Re_c = 6x10^6$ case. The present Navier-Stokes approach predicts results nearly identical to the boundary layer approach. The peak in skin friction on the lower surface is slightly higher than the boundary layer approach but both methods predict the onset of transition much better than the e^n method. The skin friction in the turbulent region is slightly better predicted than the boundary layer approach for the upper surface and slightly worse than the boundary layer approach for the lower surface. Figure 8 presents the results for the $Re_c = 2x10^6$ case. Again, the present Navier-Stokes approach predicts nearly identical transition onset locations when compared with the boundary layer approach. The Navier-Stokes approach does a slightly better job on the upper surface but both Navier-Stokes and boundary layer approaches over-predict the skin friction for the lower surface in the turbulent region. Figure 9 presents the results for the $Re_c = 0.6x10^6$ case. For

this case the boundary layer approach was not able to proceed past the separation point. The Navier-Stokes approach, however, was able to calculate the transitional and turbulent regions. In contrast to the e^n method, the present method is able to predict transition onset for the upper surface without fixing the location at the separation point. This is because the present Navier-Stokes calculations do not predict separation on the upper surface. Transition onset in the present method is fixed by the separation point for the lower surface.

Conclusions

The current results demonstrate that the present approach addresses those aspects of the breakdown process that follow the growth of linear disturbances. The e^n method is based on the conjecture that there is a critical amplification factor of the Tollmien-Schlichting waves at transition. The current approach does not support this conjecture. A key finding of the current results is that the most amplified frequency plays a major role in determining the onset of transition. Current results show that the method is an inexpensive alternative to the e^n method and provides promising transition onset prediction capabilities for a range of Reynolds numbers and freestream intensities.

Acknowledgments

This work is supported in part by NASA Grant NAG-1-244. Part of the computations were carried out at the North Carolina Supercomputing Center. The authors would like to acknowledge helpful discussions with Dr. Ndaona Chokani of North Carolina State University.

References

[1] Saric, W. S. "Physical Description of Boundary Layer Transition: Experimental Evidence". AGARD Rept. 793, March 1993.

[2] Arnal, D. "Boundary Layer Transition: Prediction, Application to Drag Reduction". AGARD Rept. 786, March 1992.

[3] Herbert, T. "Parabolized Stability Equations". AGARD Rept. 794, March 1993.

[4] Robinson, D. F., Harris, J. E., and Hassan, H. A. "Unified Turbulence Closure Model for Axisymmetric and Planar Free Shear Flows". *AIAA Journal*, Vol. 33(No. 12):2325–2331, December 1995.

[5] Robinson, D.F., and Hassan, H.A. "A Two Equation Turbulence Closure Model for Wall Bounded and Free Shear Flows". AIAA Paper 96-2057, June 1996.

[6] Obremski, H. J., Morkovin, M. V., and Landahl, M. "Portfolio of Stability Characteristics of Incompressible Boundary Layers". AGARDograph 134, Mar. 1969.

[7] Walker, G. J. "Transitional Flow on Axial Turbomachine Blading". *AIAA Journal*, Vol. 27(5):595–602, May 1989.

[8] Dhawan, S. and Narasimha, R. "Some Properties of Boundary Layer Flow During Transition from Laminar to Turbulent Motion". *Journal of Fluid Mechanics*, 3(4):418–436, 1958.

[9] Harris, J. E., and Blanchard, D. K. "Computer Program for Solving Laminar, Transitional, or Turbulent Compressible Boundary-Layer Equations for Two-Dimensional and Axisymmetric Flow". NASA TM 83207, NASA Langley, February 1982.

[10] Macaraeg, M.G., Street, G.L., and Hussaini, M.Y. "A Spectral Collocation Solution to the Compressible Stability Eigenvalue Problem". NACA Technical Paper 2858, December 1988.

[11] Schubauer, G.B., and Klebanoff, P.S. "Contributions on the Mechanics of Boundary-Layer Transition ". NACA Report 1289, 1956.

[12] Schubauer, G.B., and Skramstad, H.K. "Laminar Boundary Layer Oscillations and Transition on a Flat Plate ". NACA Report 909, 1948.

[13] Mateer, G. G., Monson, D. J., and Menter, F. R. "Skin-Friction Measurements and Calculations on a Lifting Airfoil". *AIAA Journal*, Vol. 34(No. 2):231–236, February 1996.

[14] Menter, F. R. "Two-Equation Eddy-Viscosity Turbulence Models for Engineering Applications". *AIAA Journal*, Vol. 32(No. 8):1598–1605, 1994.

Tables

Constants	$k-\zeta$
C_μ	0.09
κ	0.41
α_3	0.35
β_3	0.77
β_4	0.42
β_5	2.37
β_6	0.10
β_7	0.75
β_8	1.15
σ_r	2.00
$\frac{1}{\sigma_k}$	1.80
$\frac{1}{\sigma_\zeta}$	1.46
C_{μ_1}	4.0
C_{μ_2}	40.0
δ	0.1

Table 1: $k-\zeta$ Model Constants

Case	Tu	X_t (Experiment)	X_t (Current Method)	Error (%)
Schubauer-Klebanoff	0.03	5.26 ft.	5.39 ft.	2.47
Schubauer-Skramstad	0.042	5.25 ft.	5.24 ft.	0.19
Schubauer-Skramstad	0.10	5.08 ft.	4.86 ft.	4.3
Schubauer-Skramstad	0.20	4.05 ft.	4.08 ft.	0.74
Schubauer-Skramstad	0.26	3.32 ft.	3.41 ft.	2.7
Schubauer-Skramstad	0.34	2.58 ft.	2.52 ft.	2.3

Table 2: Flat Plate Experiments, $M_{ref} = 0.071$, $P_{ref} = 1.01325x10^5$ Pa, $T_{ref} = 293$ K.

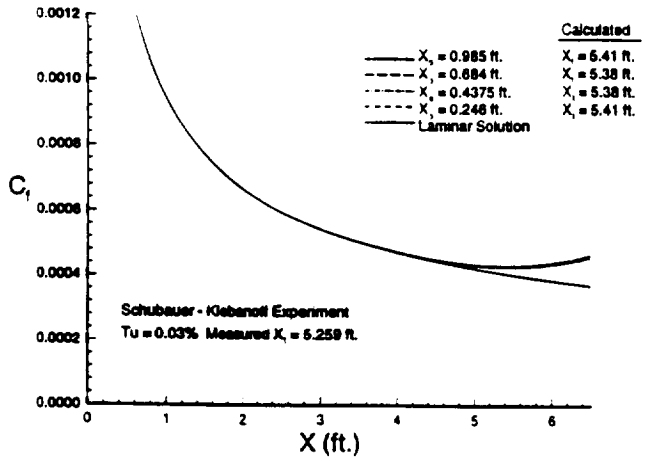

Figure 2: Effect of Initial Solution on Transition Onset, Comparison with Experiment of Ref. [11]

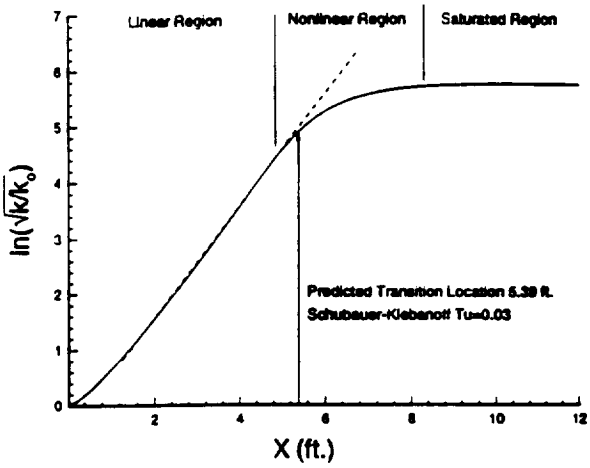

Figure 4: Amplitude ratio versus distance along plate, Schubauer-Klebanoff Experiment

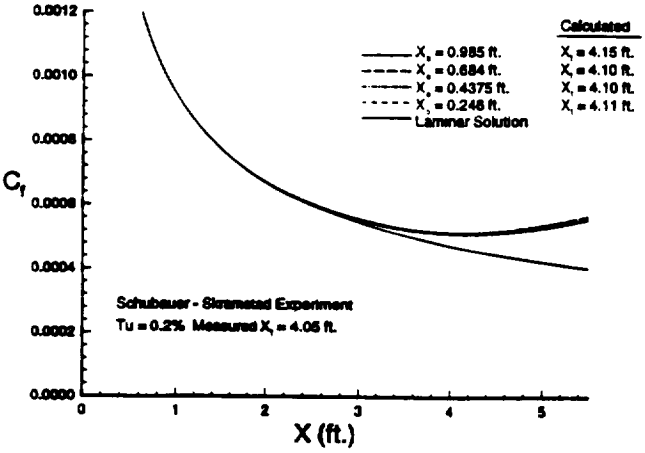

Figure 3: Effect of Initial Solution on Transition Onset, Comparison with Experiment of Ref. [12]

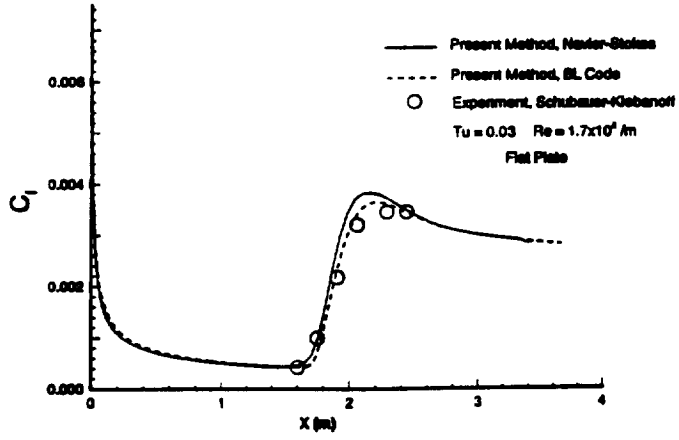

Figure 5: Comparison of present method with the experiment of Schubauer and Klebanoff, $Re = 1.67x10^6/\mathrm{m}$, Navier-Stokes & Boundary Layer Codes

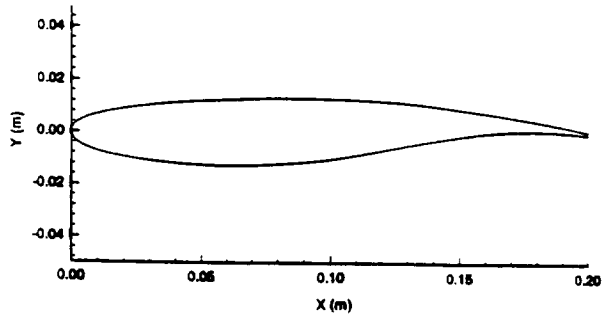

Figure 6: Airfoil geometry for experiment of Mateer et al.[13]

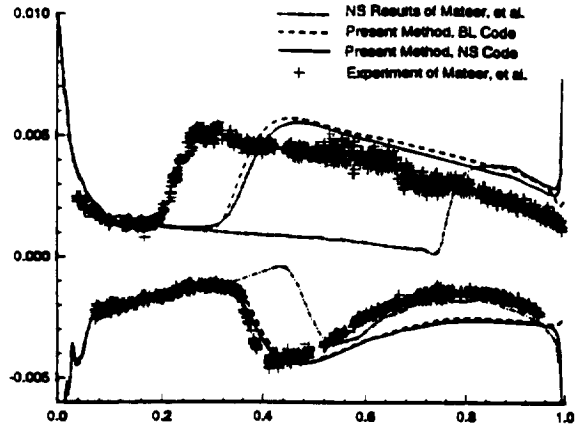

Figure 8: Comparison of present method and e^n method with the airfoil experiment of Mateer et al.[13] , $Re_c = 2$ million

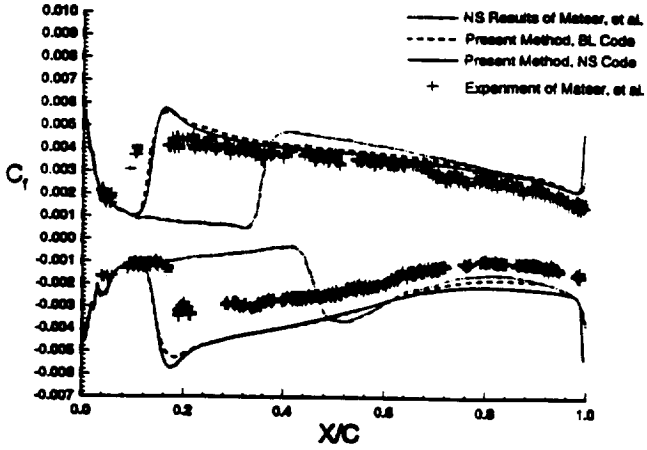

Figure 7: Comparison of present method and e^n method with the airfoil experiment of Mateer et al.[13] , $Re_c = 6$ million

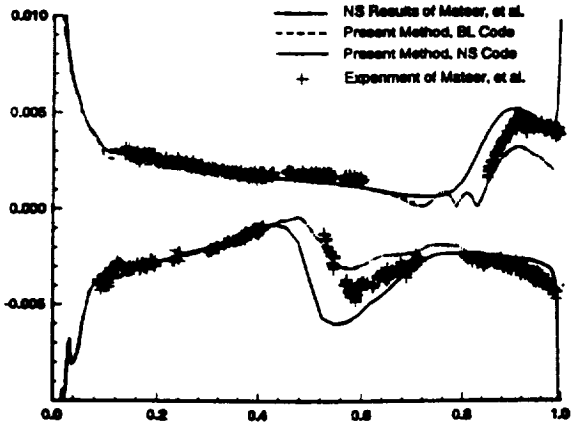

Figure 9: Comparison of present method and e^n method with the airfoil experiment of Mateer et al.[13] , $Re_c = .6$ million

AIAA 97–2245

A Transition Model for Swept Wing Flows

E. S. Warren and H. A. Hassan
North Carolina State University, Raleigh, NC

15th AIAA Applied Aerodynamics Conference
June 23–25, 1997/Atlanta, GA

A Transition Model for Swept Wing Flows

E. S. Warren* and H. A. Hassan†
North Carolina State University, Raleigh, NC

Abstract

An approach developed earlier by the authors for determining transition onset resulting from instability of Tollmien-Schlichting waves is extended to crossflow instabilities. In this approach, a two-equation model similar to that used in turbulent flows is employed. The theory takes into consideration the role of two major environmental influences: turbulence intensity and surface roughness. Comparisons with data for an infinite swept wing and an infinite swept plate under the influence of a favorable pressure gradient shows excellent agreement with experiment. Calculations employed a boundary layer code; as a result, computational costs are minimal.

Introduction

IT is well known[1,2] that the dominant mode of instability for the majority of swept-wing flows is the crossflow instability. The boundary layer on wings of moderate or greater sweep generally contains significant crossflow. The velocity profile in this case can be separated into a component in the streamwise direction and a component in the crossflow direction. Since the crossflow profile always contains an inflection point, a strong inflectional instability is expected in regions where the crossflow velocity increases rapidly.[3] This increase occurs in regions of negative pressure gradient, e.g. near the leading edge. In this favorable pressure gradient region, streamwise or Tollmien-Schlichting (T-S) instabilities are stabilized and the crossflow (CF) instability dominates the transition process.

Methods employed in transition prediction are discussed in detail by Haynes et al.[4] The practical methods that are in current use are the e^n method, which is based on linear stability theory (LST) and methods based on the parabolized stability equations (PSE). It is generally concluded that the e^n method is not suited for predicting transition onset resulting from CF instabilities. This is because these instabilities are sensitive to surface roughness, and because they are dominated during their development by large nonlinear effects that extend over a wide region. As a result, growth rates are not well predicted. Even if such rates were known, the variety of methods used to calculate the n factor result in a great deal of scatter.[3] The nonlinear PSE method[5] does a much better job of predicting growth rates if the disturbance inputs are known. Because such inputs for flight conditions and wind tunnels are not well known, its success in predicting transition onset from CF instabilities is yet to be demonstrated.

In most cases, the only data available is the turbulence intensity and very little information is provided on amplitude or frequencies of the various modes that may be present. In addition, stability analyses make use of a number of codes and require a great deal of knowledge and skill on the part of the user. Recognizing the importance of determining the onset of transition over a wide range of operating conditions for a vehicle designer, and in an effort to simplify the procedure for calculating such onset, an approach similar to that used in studying turbulence was developed by Warren and Hassan.[6] It was demonstrated in situations where T-S waves played the major role in affecting transition. The approach required knowledge of turbulence intensity and was implemented in both boundary layer and Navier-Stokes codes. Its development was based on the observation that, if a flow property can be written as the sum of mean and fluctuating components, then the exact equations governing the variance of velocity (kinetic energy of fluctuations) and the variance of vorticity (enstrophy) are the same irrespective of the nature of the fluctuations. Moreover, if such equations can be modeled without declaring the nature of fluctuations, the resulting equations are capable of describing all types of fluctuations in a fluid flow, i.e. laminar, transitional or turbulent. What distinguishes one type of fluctuation from another is the appropriate stress-strain law required to close the resulting system of equations.

The objective of this work is to extend the approach of Ref. 6 to crossflow instabilities. In order to incorporate the procedure within existing computational fluid dynamics (CFD) codes, we opted to employ an eddy viscosity model. For such models, eddy viscosity can be written as

$$\nu_t \propto k\, \tau_{tr} \tag{1}$$

where k is the fluctuation kinetic energy per unit mass and τ_{tr} is an appropriate time scale. In Ref. 6, τ_{tr} was related to the frequency of the most amplified waves. In the present case, τ_{tr} was obtained from the

*Research Assistant, Mechanical and Aerospace Engineering, Student Member AIAA.

†Professor, Mechanical and Aerospace Engineering, Associate Fellow AIAA.

observation that the wavelength of stationary crossflow vortices lies in the range of three to four times the boundary layer thickness, δ. As a result, τ_{tr} was chosen as

$$\tau_{tr} \propto \frac{3.5\,\delta}{Q_e} \tag{2}$$

where Q_e is the streamwise velocity at the edge of the boundary layer. As is shown below, the proportionality model constant depends on both the turbulent intensity and surface roughness. These are the two most dominant environmental factors that affect transition.[1]

Determining the onset of transition does not pose a problem from a computational standpoint; it does, however, represent a problem from an experimental standpoint. The data used in the validation of this method is that of Saric[1] and his colleagues and of Bippes[7] and his colleagues. The first group employed napthalene flow visualization while the second group defined onset where the intermittency is 50%. Because visualization data is somewhat subjective, the latter criterion is used in this work to facilitate comparison with experiment.

There is one important difference in implementation between this work and that of Ref. 6. In Ref. 6, the method was implemented in both boundary layer and Navier-Stokes codes because skin friction data[8] was available to validate both transition onset and flowfield calculations. Thus, the codes calculated the laminar, transitional, and turbulent regions in a single computation without interference from the user. Because flows being considered were attached, implementation was limited to a three-dimensional boundary layer code suited for calculation of infinite wings. The code is a modification of an earlier code by Harris and Blanchard.[9]

Model Formulation

The present method takes advantage of the fact that whether one deals with transition or turbulence, each flow quantity is set as a sum of a mean and fluctuating component. Moreover, the exact equations that govern the fluctuations are the same irrespective of the nature of the fluctuations. In the work of Robinson and Hassan,[10] the exact equations governing the variance of velocity (kinetic energy of fluctuations) and the variance of vorticity (enstrophy) were modeled without making use of the fact that the flow was turbulent. Therefore, the modeled equations apply to flows of any nature, whether laminar, transitional, or turbulent. In order to apply the modeled equations, it is necessary to specify a "stress-strain relationship." Following the same method used in Warren and Hassan,[6] the present approach for including crossflow instabilities is based on the modeled equations of Ref. 11 with different "stress-strain relations." The equations for the kinetic energy and enstrophy of Ref. 11 are re-written for low-speed and favorable pressure gradient flows as

$$\frac{Dk}{Dt} = -\overline{u_i' u_j'}\frac{\partial U_i}{\partial x_j} - \frac{k}{\tau_k} + \frac{\partial}{\partial x_j}\left[\left(\frac{\nu}{3} + \frac{\nu_t}{\sigma_k}\right)\frac{\partial k}{\partial x_j}\right] \tag{3}$$

$$\begin{aligned}\frac{D\zeta}{Dt} &= \frac{\partial \Omega_i}{\partial x_j}\left(\frac{\nu_t}{\sigma_r}\left[\frac{\partial \Omega_i}{\partial x_j} + \frac{\partial \Omega_j}{\partial x_i}\right]\right. \\ &\quad \left. -\epsilon_{mij}\left[\frac{\partial\left(\overline{u_m' u_l'}\right)}{\partial x_l} - \frac{\partial k}{\partial x_m}\right]\right) \\ &\quad + \frac{\partial}{\partial x_j}\left[\left(\nu + \frac{\nu_t}{\sigma_\zeta}\right)\frac{\partial \zeta}{\partial x_j}\right] - \frac{\beta_5}{R_k + \delta}\zeta^{\frac{3}{2}} \\ &\quad + \left(\alpha_3 \zeta b_{ij} + \frac{2}{3}\delta_{ij}\zeta\right) S_{ij} - \frac{\zeta \tau_{ij}\Omega_i\Omega_j\beta_4}{\rho k \Omega} \\ &\quad + 2\epsilon_{ilm}\beta_8\left(\frac{\tau_{ij}}{\rho k}\right)\left(\frac{\partial k}{\partial x_l}\frac{\partial \zeta}{\partial x_m}\right)\frac{\Omega_j}{S^2} \\ &\quad - \frac{2\beta_6 \tau_{ij}\nu_t}{\rho k \nu}\Omega\Omega_i\Omega_j + \frac{\beta_7 \zeta}{\Omega^2}\Omega_i\Omega_j S_{ij}\end{aligned} \tag{4}$$

where

$$R_k = \frac{k}{\nu\sqrt{\zeta}},\quad \nu_t = \frac{\mu_t}{\rho},\quad S = \sqrt{S_{ij}S_{ij}},\quad \Omega = \sqrt{\Omega_i\Omega_i}$$

$$R_T = \frac{k^2}{\nu\zeta},\quad \zeta = \overline{\omega_i'\omega_i'},\quad \omega_i' = \epsilon_{ilm}\partial_l u_m',\quad \Omega_i = \epsilon_{ilm}\partial_l U_m$$

and,

$$\tau_{ij} = -\overline{\rho u_i' u_j'} = \mu_t\left(2\,S_{ij} - \frac{2}{3}\delta_{ij}\frac{\partial U_m}{\partial x_m}\right) - \frac{2}{3}\rho k \delta_{ij} \tag{5}$$

τ_k is a representative decay time for the kinetic energy and ν_t is the kinematic eddy viscosity. The closure coefficients for the model are given in Table 1.

As may be seen from the governing equations, one needs to specify ν_t and τ_k to effect closure. Following the same approach as Ref. 6, the current work develops expressions for ν_t and τ_k in the laminar region. Using the concept of intermittency, the laminar expressions for ν_t and τ_k are blended with the turbulent expressions developed in the work of Robinson and Hassan.[12] A schematic of the approach is shown in Figure 1.

The eddy viscosity resulting from fluctuations in the laminar region is written as

$$\nu_t = C_\mu\, k\, \tau_{\mu_\ell},\quad C_\mu = 0.09 \tag{6}$$

where τ_{μ_ℓ} is a viscosity time scale which characterizes the dominant disturbance in the laminar region. Ref. 6 only considered the streamwise or T-S instability. Using a correlation by Walker[13] for the dominant T-S

Constants	$k-\zeta$
C_μ	0.09
κ	0.40
α_3	0.35
β_4	0.42
β_5	2.37
β_6	0.10
β_7	1.50
β_8	2.30
σ_r	0.07
$\frac{1}{\sigma_k}$	1.80
$\frac{1}{\sigma_\zeta}$	1.46
δ	0.1

Table 1 $k-\zeta$ model constants

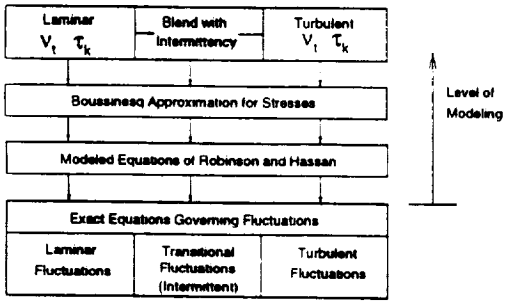

Fig. 1 Schematic of modeling objectives in present work

disturbance frequency, ω, the dominant time scale for the $T-S$ disturbances was modeled as

$$\tau_{\mu_{\ell,TS}} = \frac{a}{\omega} \tag{7}$$

where a is a model constant given in Ref. 6. The expression for a is rewritten here as

$$a = 0.00819 + 0.069\,(Tu - 0.138)^2 \tag{8}$$

and the freestream intensity, Tu, is defined as

$$Tu = 100\sqrt{\frac{2}{3}\frac{k_\infty}{Q_\infty^2}} \tag{9}$$

In contrast to Ref. 6, the current work develops a viscosity time scale which characterizes only crossflow disturbances. As discussed in Refs. 1, 2, 7, and 14, the wavelength of the dominant crossflow disturbance varies with the boundary layer thickness, δ. In addition to freestream disturbance levels, crossflow instabilities are sensitive to surface roughness. Using this information, the present method models the viscosity time scale for the crossflow instabilities as

$$\tau_{\mu_{\ell,CF}} = (a + f)\frac{\lambda_{CF}}{Q_e} \tag{10}$$

where a is the model constant given by Eq. (8) and f is a model constant which depends upon surface roughness. Q_e is the resultant boundary layer edge velocity. λ_{CF} is the wavelength of the crossflow disturbances and has been shown by Arnal[2] and other researchers to be between three and four times the boundary layer thickness, δ. Additionally, the work of Müller and Bippes[15] demonstrated that the wavelengths of both traveling and stationary crossflow disturbances were the same but shifted in phase by $\lambda_{CF}/2$. Choosing

$$\lambda_{CF} \approx 3.5\,\delta$$

the viscosity time scale in the laminar region is modeled in the present work as

$$\tau_{\mu_{\ell,CF}} = (a + f)\frac{3.5\,\delta}{Q_e} \tag{11}$$

The expression for τ_{k_ℓ} is the same form as in Ref. 6 with the addition of the roughness constant f,

$$\frac{1}{\tau_{k_\ell}} = (a + f)\frac{\nu_t}{\nu}S \tag{12}$$

Following the work of Robinson and Hassan,[11] the turbulent region time scales are given as

$$\tau_{\mu_t} = \tau_{k_t} = \frac{k}{\nu\zeta} \tag{13}$$

As in Ref. 6, the laminar and turbulent regions are combined through the intermittency, Γ. This allows a transitional eddy viscosity to be written as,

$$\nu_t = C_\mu\, k\, \tau_\mu \tag{14}$$

where

$$\tau_\mu = (1-\Gamma)\left[(a + f)\frac{3.5\,\delta}{Q_e}\right] + \Gamma\left(\frac{k}{\nu\zeta}\right) \tag{15}$$

Following a similar approach, the transitional decay time for the kinetic energy can be written

$$\frac{1}{\tau_k} = (1-\Gamma)\left[(a + f)\frac{\nu_t}{\nu}S\right] + \Gamma\left(\frac{\nu\zeta}{k}\right) \tag{16}$$

The intermittency, Γ, is currently given by the Narasimha et al.[16] expression

$$\Gamma(x) = 1 - \exp\left(-0.412\,\xi^2\right) \tag{17}$$

with

$$\xi = \max(x - x_t, 0)/\lambda \tag{18}$$

where λ characterizes the extent of the transitional region. An experimental correlation between λ and x_t is

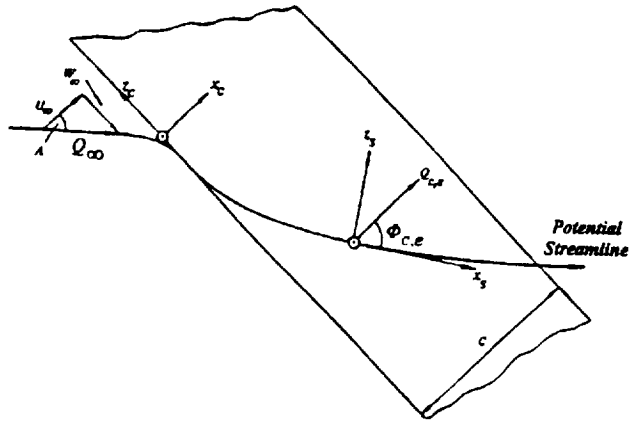

Fig. 2 Coordinate system on the swept wing and flat plate

$$Re_\lambda = 9.0 Re_{x_t}^{0.75} \tag{19}$$

x_t in the above expression represents the location where turbulent spots first appear. The present work determines x_t by the same method used in Ref. 6. In that work, it was shown that the minimum skin friction occurred when the fluctuation Reynolds number, R_T, exceeded one. R_T is defined as

$$R_T = \frac{1}{C_\mu}\frac{\nu_t}{\nu} \tag{20}$$

Thus x_t is the minimum location where $R_T \geq 1$.

Results and Discussion

The present method is compared with the swept-wing experiments of Dagenhart et al.[14] and Radeztsky et al.[17] as well as the swept flat plate experiments of Müller and Bippes[15] and Deyhle and Bippes.[7] Each of these experiments simulated infinite wing flow conditions. The infinite swept wing assumption of zero spanwise gradients was applied to the governing three-dimensional boundary-layer equations[18] and the equations governing the fluctuations, Eqs. (3) and (5). The resulting equations were then solved using a modified version of the boundary-layer code of Harris and Blanchard.[9] The necessary pressure distribution was given in the swept plate experiments and was computed from an Euler solver for the swept wing cases. The initial k profile was set from the freestream intensity, Tu, of the experiments.[6] Figure 2 shows the coordinate system used for the swept wing and swept plate geometries.

The infinite swept-wing experiments of Dagenhart et al.[14] and Radeztsky et al.[17] were carried out on a 45° swept wing with a NLF(2)–0415 airfoil cross-section at a −4° angle of attack. Figure 3 illustrates the NLF(2)–0415 profile and compares the experimental pressure coefficient on the upper surface with the computed results used in the present study. Transition onset was determined by napthalene flow visualization. As described in Dagenhart,[19] transition was determined by observing the sublimation pattern of the napthalene spray on the painted airfoil surface. The sublimation indicated higher shear levels characteristic of the transitional and turbulent regions. Traditionally, onset of transition is defined by a minimum skin friction coefficient or minimum heat transfer coefficient. However, for comparisons with available data, it is assumed that the experimentally observed transition points reported in Ref. 17 actually occurred at locations within the transitional region, i.e. non-zero intermittency. The swept flat plate experiments of Refs. 7 and 15 measured intermittency and defined transition as the location where $\Gamma = 0.5$. It is assumed, for convenience, that the data reported in the work of Radeztsky et al.[17] corresponded to a location where $\Gamma = 0.5$ as well.

The experiments reported in Radeztsky et al.[17] were carried out over a range of Reynolds numbers with three different model surface finishes. The $9\mu m$ case was the original painted finish of Dagenhart et al.[14] and is a "peak-to-peak" measured roughness of the surface finish.[17] The $0.25\mu m$ and $0.5\mu m$ cases are root-mean-squared (rms) measured roughness of the surface finish. By comparing with these cases for a given chord Reynolds number, the model constant f in Eq. (11) is correlated with roughness as is given as

$$f = 0.003\left[\left(\frac{h}{h_{ref}}\right)^{-0.8} Re_h - 0.92\right] \tag{21}$$

where

$$h_{ref} = 1\mu m$$
$$Re_h = \frac{Q_\infty h}{\nu_\infty}$$

h is the "peak-to-peak" distributed roughness level (finish). For rms measured levels, a sinusoidal distribution is assumed and the level is increased by a factor of $\sqrt{2}$. These calculations assume a freestream intensity level, $Tu = 0.09$, reported by Dagenhart.[19]

Figure 4 compares the experimental transition locations with the location of $\Gamma = 0.5$ as computed by the present method. Excellent agreement is observed for all Reynolds numbers and for all three surface finishes.

To further validate the expression for the model constant f, the present approach was used to compare with the swept flat-plate experiments of Müller and Bippes,[15] and Deyhle and Bippes.[7] The reported experiments were carried out in three different wind tunnels, designated as NWB, 1MK, and NWG. The NWB had a freestream intensity level of $Tu = 0.08$, the 1MK had values of $Tu = 0.15$ and $Tu = 0.27$ depending on whether or not a screen was present, and the NWG had an intensity of $Tu = 0.57$. Several plates of varying surface roughness were tested. Transition was determined in the experiment by increasing the effective freestream velocity until an intermittency of 50% was

Facility	Tu	Plate Surface	Experimental $Re_{x,tr}$ (x10^5)	Present $Re_{x,tr}$ (x10^5)	Error (%)
NWB	0.08	Wooden plate, $\overline{R}_z = 6\mu m$	6.5	8.04	23.7
1MK	0.15	Plate with sandpaper, $\overline{R}_z = 40\mu m$	6.8	6.12	10.0
		Wooden plate,$\overline{R}_z = 6\mu m$	7.5	7.49	0.13
		Aluminum plate, sanded, $\overline{R}_z = 5\mu m$	7.7	7.63	0.9
		Aluminum plate, polished, $\overline{R}_z = 1.8\mu m$	8.3	8.48	2.17
1MK/screen	0.27	Aluminum plate, polished, $\overline{R}_z = 1.8\mu m$	7.8	7.11	8.85
NWG	0.57	Aluminum plate, sanded, $\overline{R}_z = 5\mu m$	5.4	2.18	59.6

Table 2 Comparison of $Re_{x_c,tr}$ values at 50% intermittency predicted by the present method and measured in the swept plate experiments of Deyhle and Bippes.[7]

observed at the measurement station x_c/c=0.9. The crossflow instability was isolated in the experiment by imposing a negative pressure gradient along the plate. The pressure coefficient measured in the experiment is shown in Figure 5 for the three tunnels.

Table 2 compares the predictions of the current method with the experimental results given in Ref. 7. As seen from the table, the present approach does an excellent job of predicting the transition locations for the 1MK tunnel. Transition locations are predicted within experimental error for all intensities and surface conditions in the 1MK tunnel. The predictions by the present method were not as good for the NWB case and the transition location for the high-intensity NWG case was severely underpredicted. As discussed in Ref. 7, the $Tu = 0.57$ case could have been characterized by by-pass effects. It is also possible that the correlation for a, which was was obtained based on transition resulting from T-S instabilities, may not be appropriate for CF instabilities. We have no logical explanation as to the cause of discrepancy in the NWB tunnel. It is worth mentioning that the environmental conditions in the tunnel are comparable to those of the Arizona State University tunnel.[14,17]

Figure 6 compares the calculation of the intermittency, Γ, predicted by the present method at x_c/c=0.9 versus Reynolds number. As seen from the figure, the present method compares well with the experimental data.

In Ref. 15, first turbulent spots were detected at location x_c/c=0.95 for the $6\mu m$ plate in the 1MK tunnel at $Tu = 0.15$ and $Q_\infty = 19m/s$. The location of first turbulent spots is the definition of x_t in Eq. (18) and the present method predicts this location at x_c/c=0.949 giving excellent agreement with Ref. 15.

The rms amplitude of the *total* velocity disturbance can be obtained from the kinetic energy of the fluctuations as,

$$A = \sqrt{k} = \sqrt{\frac{\overline{u'^2 + v'^2 + w'^2}}{2}} \qquad (22)$$

Figure 7 is a plot of the amplitude ratio for the $Tu = 0.15$ and $6\mu m$ roughness case in the 1MK tunnel. k_o in the figure represents the maximum kinetic energy of the fluctuations at the initial station in the boundary-layer marching procedure (freestream k). As seen from the figure, the present method predicts a region of linear growth and a significant region on non-linear growth as the onset of transition is approached. The disturbance level tends to saturate as onset is approached but resumes exponential growth when the transitional region is entered. This agrees qualitatively with the large eddy simulation (LES) results presented by Huai et al.[20] The ability to capture the nonlinear growth shown in Figure 7 demonstrates the sound basis of the present method.

Conclusions

It is shown in this investigation that treating transitional flows in a manner similar to turbulent flows represents a convenient and an inexpensive method for determining transition onset. The key to this approach is to determine the relevant eddy viscosity suited for describing the underlying physics of the problem.

Because of the turbulence-like approach developed here, the manner in which the various modes interact with each other and with the environment to bring about transition is integrated out of the problem. Evidently, one of the significant outcomes of the interaction is the fact that the CF disturbances have a wave length that varies between three to four times the boundary layer thickness.

Acknowledgments

This work is supported in part by NASA Grant NAG-1-1876. Part of the computations were carried out at the North Carolina Supercomputing Center. This work would not have been possible without the help and support of the following individuals: Professor Bill Saric of Arizona State University for providing us with relevant publications; Dr. Hans Bippes of the DLR for providing us with the data and for the many E-mails that helped us correctly interpret his data; Dr. Ray Dagenhart of NASA-Langley Research Center for providing us with data and for sharing with us his expertise in the field; Dr. Ron Joslin of NASA-Langley Research Center who introduced us to the subject and

explained to us its many fine points and intricacies: and Dr. Nd. Chokani of North Carolina State University for many helpful discussions and suggestions.

References

[1]Saric, W. S., "Physical Description of Boundary Layer Transition: Experimental Evidence," AGARD Report 793, March 1993.

[2]Arnal, D., "Boundary Layer Transition: Prediction, Application to Drag Reduction," AGARD Report 786, March 1992.

[3]Arnal, D., "Boundary Layer Transition: Predictions Based on Linear Theory," AGARD Report 793, April 1994.

[4]Haynes, T.S., Reed, H.L., and Saric, W.S., "CFD Validation Issues in Transition Modeling," AIAA Paper 96–2057, June 1996.

[5]Herbert, T., "Progress in Applied Transition Analysis," AIAA Paper 96–1993, June 1996.

[6]Warren, E.S., and Hassan, H.A. , "An Alternative to the e^n Method for Determining Onset of Transition," AIAA Paper 97–0825, January 1997.

[7]Deyhle, H., and Bippes, H., "Disturbance Growth in an Unstable Three-Dimensional Boundary Layer and its Dependence on Environmental Conditions," *Journal of Fluid Mechanics*, Vol. 316, June 1996, pp. 73–113.

[8]Mateer, G. G., Monson, D. J., and Menter, F. R., "Skin-Friction Measurements and Calculations on a Lifting Airfoil," *AIAA Journal*, Vol. 34, No. 2, February 1996, pp. 231–236.

[9]Harris, J. E., and Blanchard, D. K., "Computer Program for Solving Laminar, Transitional, or Turbulent Compressible Boundary-Layer Equations for Two-Dimensional and Axisymmetric Flow," NASA TM 83207, February 1982.

[10]Robinson, D. F., Harris, J. E., and Hassan, H. A., "Unified Turbulence Closure Model for Axisymmetric and Planar Free Shear Flows," *AIAA Journal*, Vol. 33, No. 12, December 1995, pp. 2325–2331.

[11]Robinson, D.F., and Hassan, H.A., "Modeling Turbulence Without Damping Functions Using $k - \zeta$ Model," AIAA Paper 97–2312, June 1997.

[12]Robinson, D.F., and Hassan, H.A., "A Two Equation Turbulence Closure Model for Wall Bounded and Free Shear Flows," AIAA Paper 96–2057, June 1996.

[13]Walker. G. J., "Transitional Flow on Axial Turbomachine Blading," *AIAA Journal*, Vol. 27, No. 5, May 1989, pp. 595–602.

[14]Dagenhart. J.R., Saric, W.S., Hoos J.A., and Mousseux. M.C., "Experiments on Swept Wing Boundary Layers," *Laminar–Turbulent Transition. IUTAM Symposium. Toulouse. France*, edited by D. Arnal and R. Michel, Springer Verlag, 1989.

[15]Müller, B., and Bippes, H., "Experimental Study of Instability Modes in a Three-Dimensional Boundary Layer," AGARD Report 438, October 1988.

[16]Dhawan, S. and Narasimha, R., "Some Properties of Boundary Layer Flow During Transition from Laminar to Turbulent Motion," *Journal of Fluid Mechanics*, Vol. 3, No. 4, 1958, pp. 418–436.

[17]Radeztsky, R.H. Jr., Reibert, M.S., Saric, W.S., and Takagi, S., "Effect of Micron-Sized Roughness on Transition in Swept-Wing Flows," AIAA Paper 93–0076, January 1993.

[18]Schlichting, H., *Boundary-Layer Theory*, McGraw-Hill, seventh ed., 1979.

[19]Dagenhart, J., *Crossflow Stability and Transition experiments in a Swept-Wing Flow*, Ph.D. thesis, Virginia Polytechnic Institute and State University, 1992.

[20]Huai, X., Joslin, R.D., "Large-Eddy Simulation of Laminar-Turbulent Transition in a Swept-Wing Boundary Layer," AIAA Paper 97–0750, January 1997.

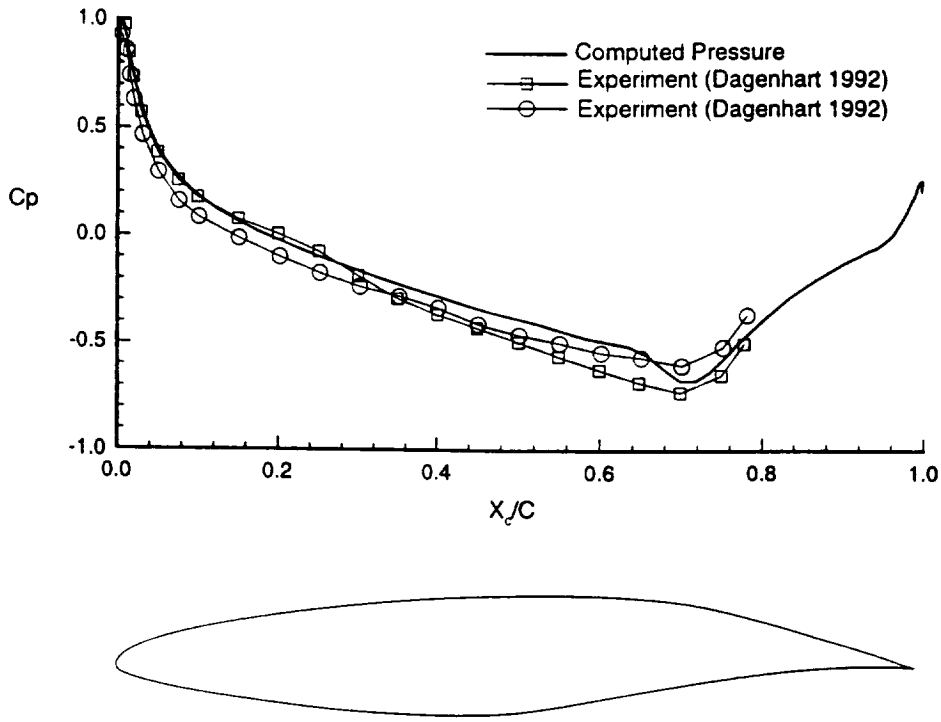

Fig. 3 NLF(2)–0415 airfoil geometry and comparison of experimental and computed pressure coefficient on the upper surface.

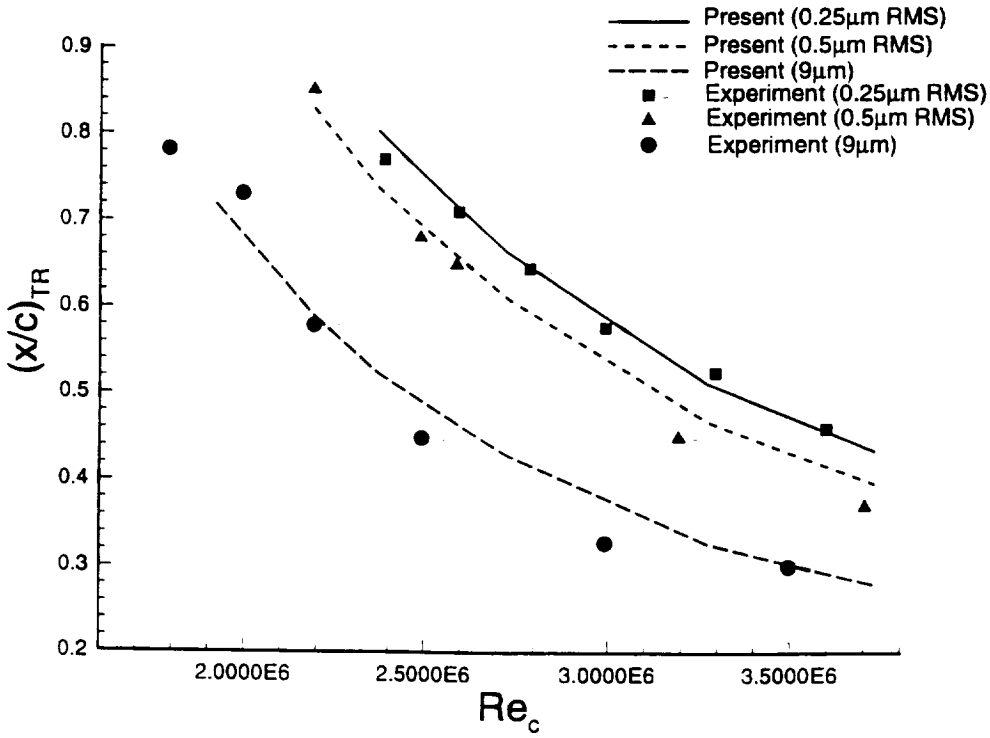

Fig. 4 Comparison of the present method with the experimental data of Radeztsky et al.[17]

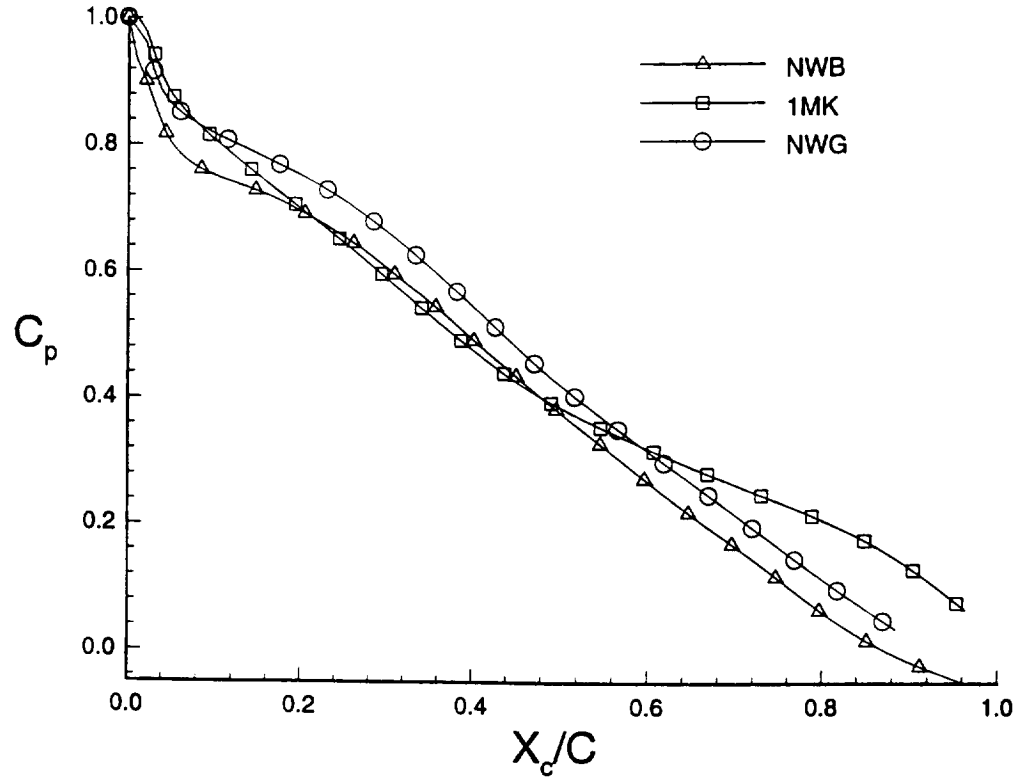

Fig. 5 Experimental pressure coefficient along the swept plate of Deyhle and Bippes[7]

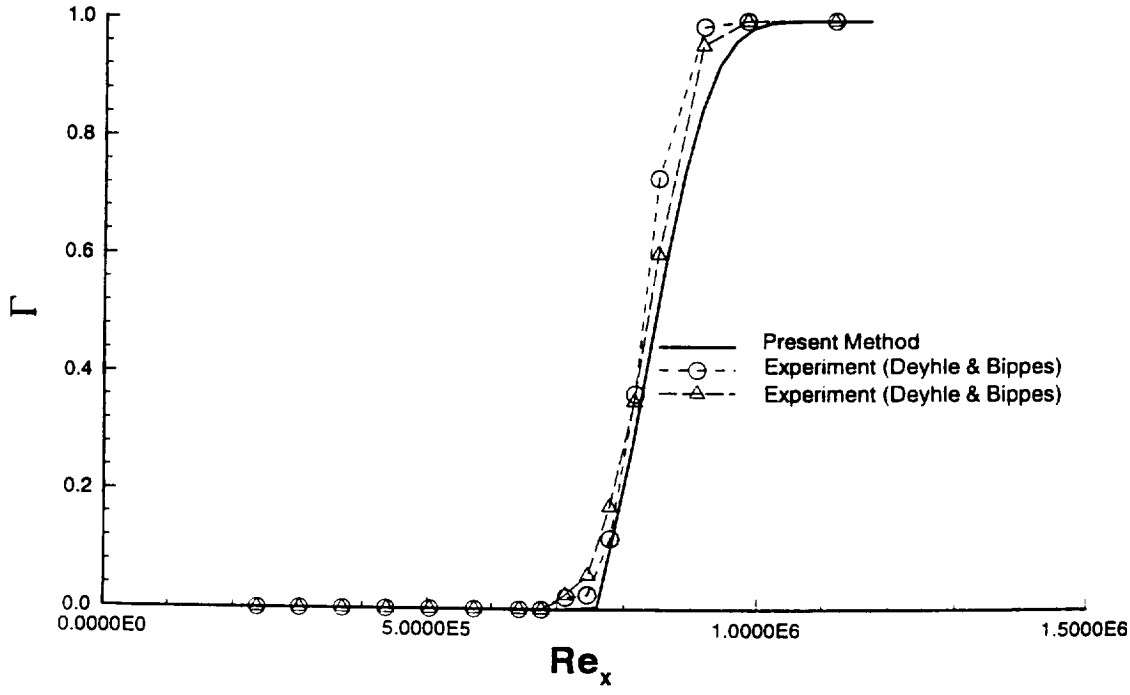

Fig. 6 Comparison of the intermittency predicted by the present method with the experimental data of Deyhle and Bippes,[7] x_c/c=0.9.

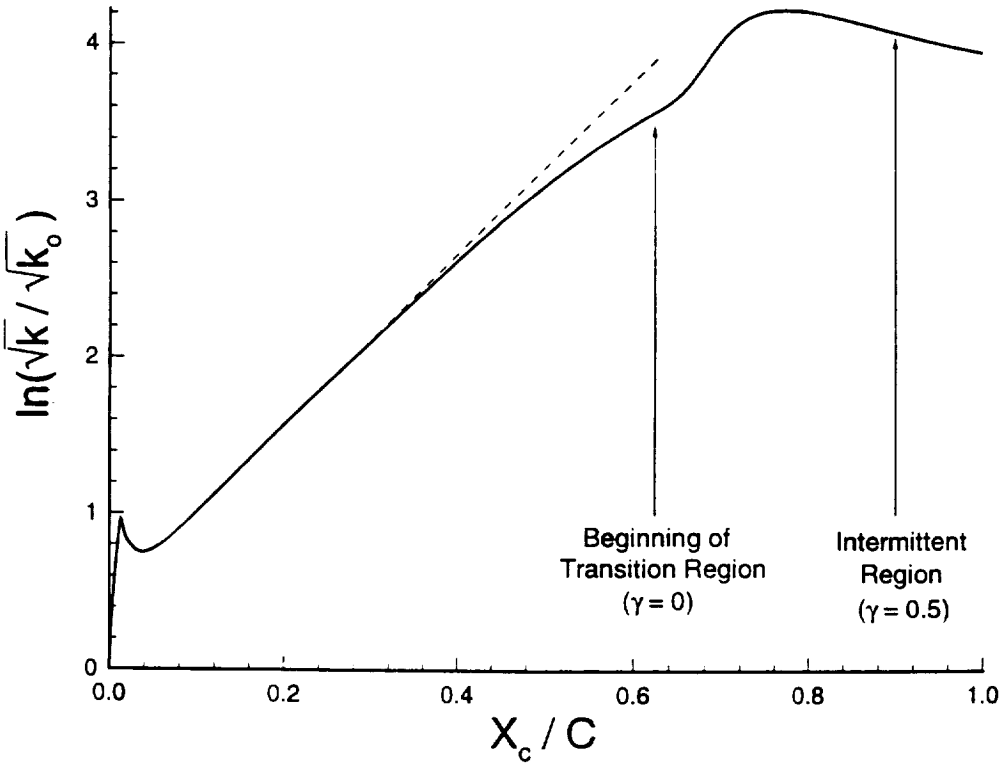

Fig. 7 Amplitude ratio versus distance, Deyhle and Bippes[7] swept plate, $Tu = 0.15$, $\overline{R}_z = 6\mu m$.

975502

A Transition Closure Model for Predicting Transition Onset

Eric S. Warren and Hassan A. Hassan
North Carolina State Univ.

1997 World Aviation Congress
October 13-16, 1997
Anaheim, CA

SAE The Engineering Society For Advancing Mobility Land Sea Air and Space INTERNATIONAL

SAE International
400 Commonwealth Drive
Warrendale, PA 15096-0001 U.S.A.

AIAA

American Institute of Aeronautic and Astronautics
370 L'Enfant Promenade, S.W.
Washington, D.C. 20024

Published by the American Institute of Aeronautics and Astronautics (AIAA) at 1801 Alexander Bell Drive, Suite 500, Reston, VA 22091 U.S.A., and the Society of Automotive Engineers (SAE) at 400 Commonwealth Drive, Warrendale, PA 15096 U.S.A.

Produced in the U.S.A. Non-U.S. purchasers are responsible for payment of any taxes required by their governments.

ISSN #0148-7191

All AIAA papers are abstracted and indexed in International Aerospace Abstracts and Aerospace Database.

All SAE papers, standards and selected books are abstracted and indexed in the Global Mobility Database.

Copies of this paper may be purchased from:

AIAA's document delivery service
Aeroplus Dispatch
1722 Gilbreth Road
Burlingame, California 94010-1305
Phone: (800) 662-2376 or (415) 259-6011
Fax: (415) 259-6047

or from:

SAExpress Global Document Service
c/o SAE Customer Sales and Satisfaction
400 Commonwealth Drive
Warrendale, PA 15096
Phone: (412) 776-4970
Fax: (412) 776-0790

SAE routinely stocks printed papers for a period of three years following date of publication. Quantity reprint rates are available.

97550

A Transition Closure Model for Predicting Transition Onset

Eric S. Warren and Hassan A. Hassan
North Carolina State Uni

ABSTRACT

A unified approach which makes it possible to determine the extent and onset of transition in one calculation is presented. It treats the laminar fluctuations in a manner similar to that used in describing turbulence. As a result, the complete flowfield can be calculated using existing CFD codes and without the use of stability codes. The method is validated by comparing the results for flat plates, airfoils, and infinite swept wings with available experiments. In general, good agreement is indicated.

INTRODUCTION

Traditionally, the transition problem has been treated as a combination of two problems. The first deals with the extent of the transition region given the onset, while the second deals with transition onset. One of the methods employed in calculating the extent is to set the effective viscosity, μ, in a boundary layer (BL) code or Navier-Stokes (NS) solver as

$$\mu = \mu_\ell + \Gamma \mu_t \tag{1}$$

where subscripts ℓ and t designate laminar and turbulent flows respectively and Γ is the intermittency or the fraction of time the flow is turbulent at a given location. The most widely used expression is that of Dhawan and Narasimha.[1]

There are many ways that are being used to specify transition onset: arbitrary selection, experimental correlations, or use of stability theory. Methods based on stability theory employ the e^n method or a method based on the parabolized stability equations (PSE). Methods based on stability theory have shown a great deal of promise when streamwise or Tollmien-Schlichting (T-S) waves are the dominant cause of transition. The same cannot be said when transition is a result of crossflow (CF) instabilities because such instabilities are dominated by nonlinear effects and surface roughness. An excellent recent review of these methods and their limitations is given by Haynes et al.[2]

In situations where transition onset is specified from results of an experiment, Eq. (1) does not perform well. One of the reasons for this behavior is because the above formula does not account for the laminar fluctuations that eventually lead to transition. This led Young et al.[3] and Warren et al.[4] to employ an expression for μ given by

$$\mu = \mu_\ell + [(1-\Gamma)\mu_{\ell f} + \Gamma \mu_t] \tag{2}$$

where $\mu_{\ell f}$ is the contribution of the laminar fluctuations. The expression for $\mu_{\ell f}$ was correlated by using results from linear stability theory for both low and high speed flows. Much better agreement with experiment was indicated when Eq. (2) was employed.

The inability of stability theory to cope with crossflow instabilities led Warren and Hassan[5,6] to develop a new approach for determining transition onset. This approach is centered around the determination of $\mu_{\ell f}$. When $\mu_{\ell f}$ is known, then the onset of transition, which may correspond to minimum skin friction, minimum heat flux, or some other criterion specified by the user, can be determined as a part of the solution. Such an approach then removes the need for stability codes to predetermine transition onset. Moreover, it addresses transition onset and extent as one and not two separate problems.

In both transition and turbulence each flow quantity is set as a sum of a mean and fluctuating quantity. The exact equations governing fluctuations are the same. In transition, attention is focused on individual modes and frequencies with the growth rates of such modes playing a crucial role in determining transition onset. In turbulence, equations governing fluctuations are used to derive equations for the mean energy of the fluctuations and its dissipation rate. As a result, individual modes do not play any direct role in turbulence calculations. The resulting equations governing turbulence are not closed, thus necessitating assumptions on a stress-strain law.

The approach presented here takes advantage of similarities between laminar and turbulent fluctuations, i.e. the exact equations governing energy and it dissipation rate are identical. Moreover, it is possible to model these exact equations[7] without invoking the nature of fluctuations. In order to close the model equations, it is necessary t

provide appropriate stress-strain laws. To facilitate implementation in existing CFD codes, an eddy viscosity model will be employed.

In the present work, the stress-strain laws for the laminar fluctuations are derived from observed or computed characteristics of T-S and CF disturbances. Because mechanisms responsible for transition are different for the two types of instabilities, corresponding stress-strain laws are different. In both cases, however, $\mu_{\ell f}$ is set as

$$\mu_{\ell f} = C_\mu \, \rho \, k \, \tau \tag{3}$$

where k is the fluctuation kinetic energy per unit mass, ρ is the density, and τ is an appropriate time scale characteristic of the type of instabilities begin considered. Although the present approach makes no direct use of stability codes, expressions for τ were arrived at from consideration of results obtained from stability theory or from experimental observations.

It is to be noted that this is not the first attempt at using equations similar to the turbulence equations to predict transition onset. Typical of these attempts is the work of Wilcox.[8-10] An earlier attempt[9] tried to take advantage of the results of linear stability theory. In the latest effort,[10] the approach used in Ref. 9 was abandoned in favor of an approach in which the model constants in the $k-\omega$ model were replaced by functions of the turbulence Reynolds number. The functions were selected in such a way so as to reduce to the original model constants at high turbulence Reynolds number and to reproduce transition onset for an incompressible flow over a flat plate. As formulated, the model is insensitive to the modes of transition[11] and thus will not yield good results outside the range for which it was formulated.[12] This may be contrasted with the present model in which separate equations are used to model the "laminar" fluctuations and where the stress-strain laws that govern those fluctuations are not only sensitive to the various modes of transition but are dictated by them.

PROBLEM FORMULATION

The basis for the present approach is the exact equations governing k and ζ, the enstrophy or the variance of vorticity. The $k-\zeta$ turbulence model employed in this work is that of Robinson and Hassan.[13] The equations governing k and ζ are those given in the work of Robinson et al.[13] and can be rewritten for low speed flows as

$$\frac{Dk}{Dt} = -\overline{u_i' u_j'}\frac{\partial U_i}{\partial x_j} - \frac{k}{\tau_k} + \frac{\partial}{\partial x_j}\left[\left(\frac{\nu}{3} + \frac{\nu_t}{\sigma_k}\right)\frac{\partial k}{\partial x_j}\right] \tag{4}$$

$$\begin{aligned}\frac{D\zeta}{Dt} &= \frac{\partial \Omega_i}{\partial x_j}\left(\frac{\nu_t}{\sigma_r}\left[\frac{\partial \Omega_i}{\partial x_j} + \frac{\partial \Omega_j}{\partial x_i}\right]\right. \\ &\quad \left. -\epsilon_{mij}\left[\frac{\partial\left(\overline{u_m' u_l'}\right)}{\partial x_l} - \frac{\partial k}{\partial x_m}\right]\right) \\ &\quad + \frac{\partial}{\partial x_j}\left[\left(\nu + \frac{\nu_t}{\sigma_\zeta}\right)\frac{\partial \zeta}{\partial x_j}\right] - \frac{\beta_5}{R_k + \delta}\zeta^{\frac{3}{2}} \\ &\quad + \left(\alpha_3 \zeta b_{ij} + \frac{2}{3}\delta_{ij}\zeta\right) S_{ij} - \frac{\zeta \tau_{ij}\Omega_i\Omega_j\beta_4}{\rho k \Omega} \\ &\quad + 2\epsilon_{ilm}\beta_8\left(\frac{\tau_{ij}}{\rho k}\right)\left(\frac{\partial k}{\partial x_l}\frac{\partial \zeta}{\partial x_m}\right)\frac{\Omega_j}{S^2} \\ &\quad - \frac{2\beta_6 \tau_{ij}\nu_t}{\rho k \nu}\Omega\Omega_i\Omega_j + \frac{\beta_7 \zeta}{\Omega^2}\Omega_i\Omega_j S_{ij} \\ &\quad + \max\left[\frac{\partial(\rho U_i P)}{\partial x_i}, 0.0\right]\frac{k\Omega}{\nu P \sigma_p}\end{aligned} \tag{5}$$

where

$$R_k = \frac{k}{\nu\sqrt{\zeta}}, \quad \nu_t = \frac{\mu_t}{\rho}, \quad S = \sqrt{S_{ij}S_{ij}}, \quad \Omega = \sqrt{\Omega_i\Omega_i}$$

$$R_T = \frac{k^2}{\nu\zeta}, \quad \zeta = \overline{\omega_i'\omega_i'}, \quad \omega_i' = \epsilon_{ilm}\partial_l u_m', \quad \Omega_i = \epsilon_{ilm}\partial_l U_m$$

$$S_{ij} = \frac{1}{2}\left[\frac{\partial U_i}{\partial x_j} + \frac{\partial U_j}{\partial x_i}\right]$$

and,

$$\tau_{ij} = -\overline{\rho u_i' u_j'} = \mu_t\left(2\,S_{ij} - \frac{2}{3}\delta_{ij}\frac{\partial U_m}{\partial x_m}\right) - \frac{2}{3}\rho k \delta_{ij} \tag{6}$$

τ_k is a representative decay time for the kinetic energy and ν_t is the kinematic eddy viscosity. The closure coefficients for the model are given in Table 1.

Table 1 $k-\zeta$ model constants

Constants	$k-\zeta$
C_μ	0.09
κ	0.40
α_3	0.35
β_4	0.42
β_5	2.37
β_6	0.10
β_7	1.50
β_8	2.30
σ_r	0.07
σ_p	0.065
$\frac{1}{\sigma_k}$	1.80
$\frac{1}{\sigma_\zeta}$	1.46
δ	0.1

As may be seen from the governing equations, one needs to specify ν_t and τ_k for each mechanism to effect closure. When T-S waves are considered, ν_t is chosen as[5]

$$\nu_t = C_\mu \, k \, \tau_{\mu_t} \tag{7}$$

where

$$\tau_{\mu_t} = \tau_{\mu_t, TS} = \frac{a}{\omega} \tag{8}$$

ω is the frequency of the first mode disturbance having the maximum amplification rate and a is a model constant that depends on the freestream intensity, Tu, defined as

$$Tu = 100\sqrt{\frac{2}{3}\frac{k_\infty}{Q_\infty^2}} \tag{9}$$

In the above expression, Q_∞ is the freestream velocity. The frequency ω is given by a correlation developed by Walker[14] as

$$\frac{\omega\nu}{Q_e^2} = 3.2 Re_{\delta^*}^{-3/2} \tag{10}$$

where Q_e is the velocity at the edge of the boundary layer and Re_{δ^*} is the edge Reynolds number based on a displacement thickness δ^*. The model constant a was correlated using flat plate experiments by Schubauer and Klebanoff[15] and Schubauer and Skramstad[16] as[5]

$$a = 0.069\,(Tu - 0.138)^2 + 0.00819 \tag{11}$$

Within the laminar region, the representative decay time for the kinetic energy is

$$\frac{1}{\tau_{k_\ell}} = a\frac{\nu_t}{\nu}S \tag{12}$$

Similarly, when transition is a result of CF instabilities[6]

$$\tau_{\mu_\ell} = \tau_{\mu_{\ell,CF}} = (a + f)\frac{\lambda_{CF}}{Q_e} \tag{13}$$

where λ_{CF} is the wavelength of crossflow disturbances. Based on numerous experimental and computational results which found wavelengths of CF disturbances between 3 and 4 times the boundary layer thickness, we use here

$$\lambda_{CF} = 3.5\,\delta \tag{14}$$

Since stationary CF disturbances are generated by surface roughness and traveling disturbances are generated by freestream disturbances and surface conditions, a correlation reflecting the influence of surface conditions must be included in the model. Using one of the sets reported by Radeztsky et al.,[17] f was correlated as[6]

$$f = 0.003\left[\left(\frac{h}{h_{ref}}\right)^{-0.8} Re_h - 0.92\right] \tag{15}$$

where

$$h_{ref} = 1\mu m \tag{16}$$

$$Re_h = \frac{Q_\infty h}{\nu_\infty} \tag{17}$$

and h is the "peak-to-peak" distributed roughness level. The decay time for the kinetic energy is chosen as

$$\frac{1}{\tau_{k_t}} = (a + f)\frac{\nu_t}{\nu}S \tag{18}$$

Following the work of Robinson and Hassan,[13] the turbulent region time scales are given by

$$\tau_{k_t} = \tau_{\mu_t} = \frac{k}{\nu\zeta} \tag{19}$$

Because the thrust of this work is the prediction of transition onset, a simple intermittency approach is used in the transition region. As a result

$$\tau_\mu = (1-\Gamma)\tau_{\mu_\ell} + \Gamma\tau_{\mu_t} \tag{20}$$

$$\frac{1}{\tau_k} = (1-\Gamma)\frac{1}{\tau_{k_\ell}} + \Gamma\frac{1}{\tau_{k_t}} \tag{21}$$

The intermittency, Γ, is given by Dhawan and Narasimha's[1] expression, i.e.

$$\Gamma(x) = 1 - \exp\left(-0.412\,\xi^2\right) \tag{22}$$

with

$$\xi = \max(x - x_t, 0)/\lambda \tag{23}$$

λ is a characteristic extent of the transitional region. An experimental correlation between λ and x_t is

$$Re_\lambda = 9.0 Re_{x_t}^{0.75} \tag{24}$$

with x_t being the location where turbulent spots first appear, or where skin friction is minimum. It is shown in the work of Warren et al.[5] that this location is well represented by the relation

$$R_T = \frac{1}{C_\mu}\frac{\nu_t}{\nu} = 1.0 \tag{25}$$

Thus, x_t is the minimum location where $R_T \geq 1$.

RESULTS AND DISCUSSION

Results presented here employed both boundary layer and Navier-Stokes codes. The boundary layer (BL) code is an adaptation of the code developed by Harris and Blanchard.[18] In addition to incorporating the present transition/turbulence model, it was extended to handle infinite swept wings. The Navier-Stokes (NS) code is an adaptation of an earlier code developed by Gaffney et al.,[19] which employs an upwind Roe scheme and four step Runge-Kutta time stepping method. When employing a boundary layer code, the pressure distribution is obtained from an Euler code or experiment.

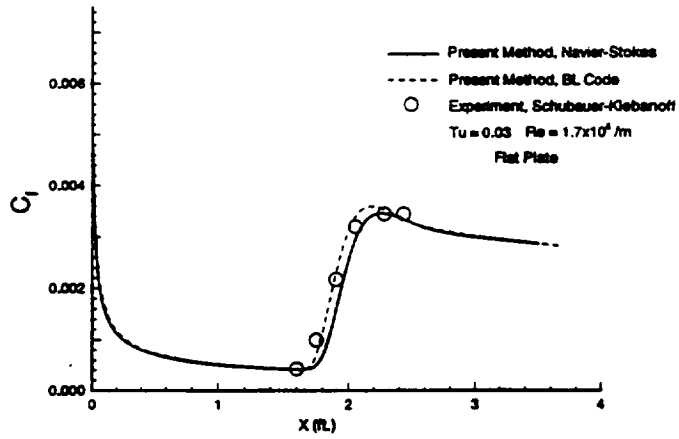

Figure 1 Comparison of present method with the experiment of Schubauer and Klebanoff, Re = 1.67 × 10^6/m, Navier-Stokes & Boundary Layer Codes

Transition resulting from T-S instabilities is discussed first. The only environmental parameter that needs to be specified is the freestream intensity. Figure 1 compares predictions of present theory with measurements over a flat plate.[15] With the current model, the only environmental condition that needs to be specified is the freestream turbulence level. Both computational schemes give similar results with regard to onset and extent of transition. The

Table 2 Flat Plate Experiments. $M_{ref} = 0.071$, $P_{ref} = 1.01325 \times 10^5$ Pa, T_{ref} 293 K.

Case	Tu	X_t (Experiment)	X_t (Current Method)	Error (%)
Schubauer-Klebanoff	0.03	5.26 ft.	5.39 ft.	2.47
Schubauer-Skramstad	0.042	5.25 ft.	5.24 ft.	0.19
Schubauer-Skramstad	0.10	5.08 ft.	4.86 ft.	4.3
Schubauer-Skramstad	0.20	4.05 ft.	4.08 ft.	0.74
Schubauer-Skramstad	0.26	3.32 ft.	3.41 ft.	2.7
Schubauer-Skramstad	0.34	2.58 ft.	2.52 ft.	2.3

transition onset locations predicted by the present method are compared with the flat pate experiments of Schubauer and Klebanoff[15] and Schubauer and Skramstad[16] in Table 2. As seen from the table, excellent results are obtained for all freestream intensities reported. The next set of comparisons involve the data of Mateer et al.[20] They presented skin friction measurements over the supercritical airfoil shown in Figure 2 for a freestream Mach number, M_∞, of

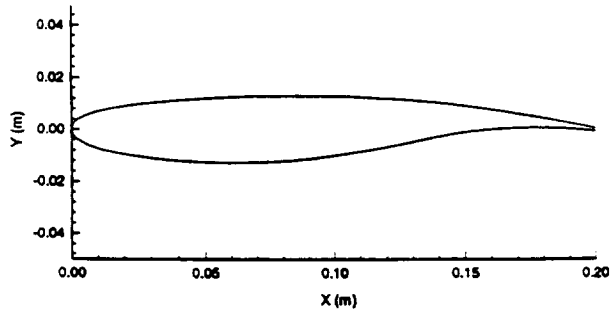

Figure 2 Airfoil geometry for experiment of Mateer et al.[20]

0.2 and a range of Reynolds numbers and angles of attack, α. Moreover, they compared their measurements with the e^n method. Emphasis will be placed on comparisons with $\alpha = -0.5°$ cases because this is the angle of attack where large discrepancies between the e^n method and experimental data were noted. It is suggested that the e^n method is incapable of predicting transition for these cases when transition is dominated by Reynolds number effects and not determined solely by laminar separation.[20]

Figs. 3–5 show a comparison of predictions of present theory with experiment and calculations reported in the work of Mateer et al.[20] Both BL and NS calculations are shown. It is to be noted that when transition is a result of flow separation, BL calculations are terminated at separation. Fig. 3 compares results for $Re_c = 0.6 \times 10^6$. For this case the e^n method sets transition on both upper and lower surfaces as the location of laminar flow separation. As may be seen from the figure, the present theory gives good agreement with experiment for both upper and lower surfaces. For $Re_c = 2 \times 10^6$, Fig. 4 shows that the present method gives much better agreement than the e^n method

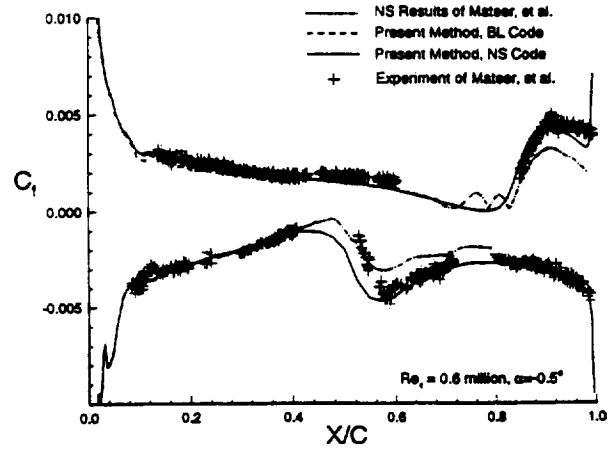

Figure 3 Comparison of present method and e^n method with the airfoil experiment of Mateer et al.[20] , $Re_c = .6$ million, $\alpha = -0.5°$

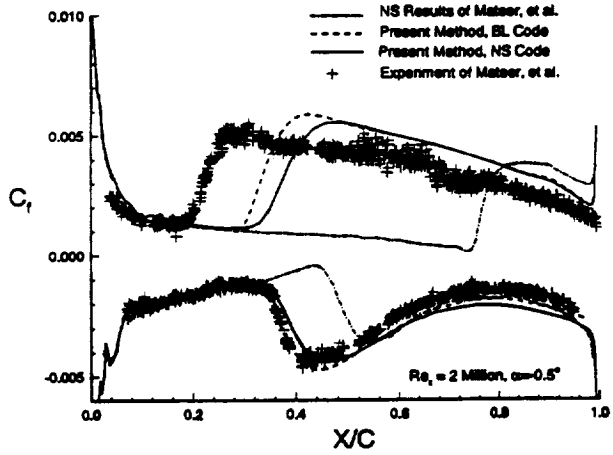

Figure 4 Comparison of present method and e^n method with the airfoil experiment of Mateer et al.[20] , $Re_c = 2$ million, $\alpha = -0.5°$

with experiment for both upper and lower surfaces. A similar conclusion is reached for $Re_c = 6 \times 10^6$ as shown in Fig. 5. It is to be noted however, that for this case, the current model overpredicts skin friction over part of the airfoil while giving reasonable estimates of onset location. It is difficult to pinpoint the cause of the discrepancy in skin friction for this case especially when good agreement for the other cases was indicated. Possible contributing factors may be the expression used to describe intermittency

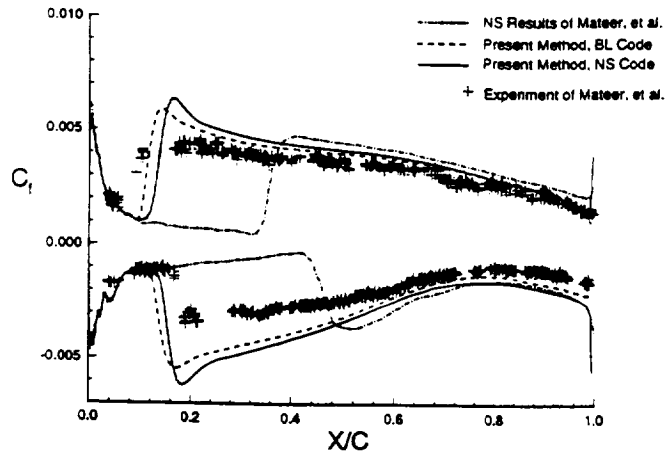

Figure 5 Comparison of present method and e^n method with the airfoil experiment of Mateer et al.[20] , $Re_c = 6$ million, $\alpha = -0.5°$

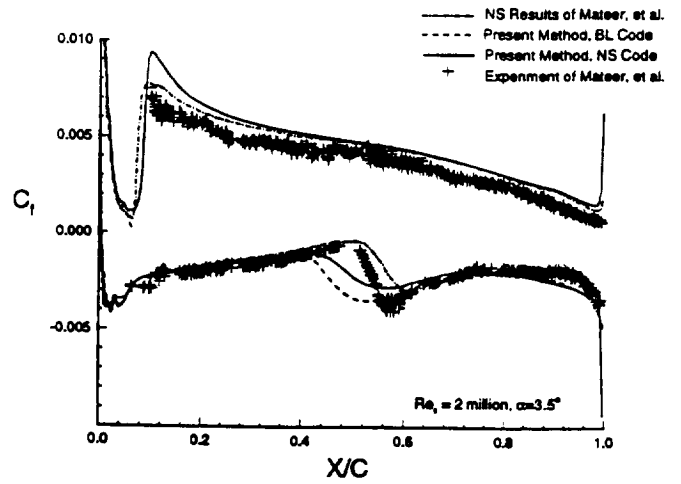

Figure 6 Comparison of present method and e^n method with the airfoil experiment of Mateer et al.[20] , $Re_c = 2$ million, $\alpha = 3.5°$

or increased blockage in the tunnel.

For higher angles of attack, the present method and e^n methods are somewhat comparable in their predictions. Figure 6 compares calculations for $\alpha = 3.5°$ and $Re_c = 2 \times 10^6$. It is to be noted that both models overestimate skin friction on the upper surface. For the upper surface, both models predict transition at the location of separation. However, for the lower surface the present method predicts a location slightly upstream of the location of laminar separation. For this case, the e^n method predicts transition at the location of laminar separation for both upper and lower surfaces.

The next set of comparisons address transition resulting from crossflow instabilities. Figure 7 shows the coordinate system used for the swept wing and swept plate geometries. For these cases, available data give transition onset locations.[17,21-23] Unfortunately, skin friction data is not provided. Moreover, flow separation does not play any role in determining transition onset in available data. As a result, computations presented for CF instabilities were

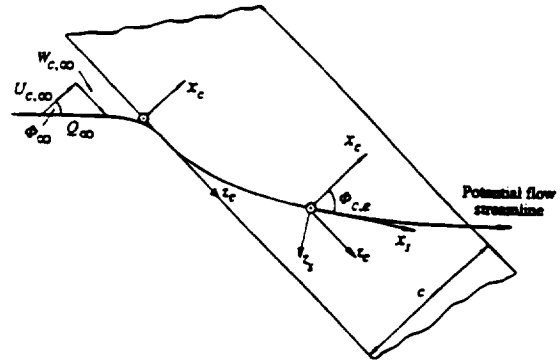

Figure 7 Coordinate system on the swept wing ar flat plate

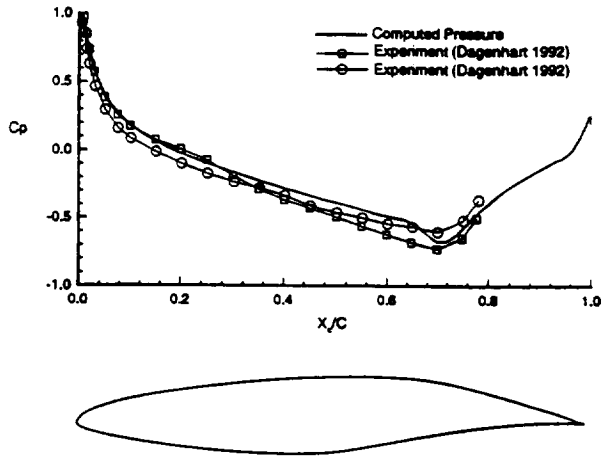

Figure 8 NLF(2)–0415 airfoil geometry and compar son of experimental and computed pressure coefficie on the upper surface.

based on a three-dimensional boundary layer code suite for calculating infinite swept wings. For such flows, tl boundary layer equations do not depend on the spanwi coordinate.[24]

The infinite swept wing experiments of Dagenhart al.[21] and Radeztsky et al.[17] use a 45° swept wing with NLF(2)-0415 cross-section at −4° angle of attack. Figure illustrates the NLF(2)–0415 profile and compares the e perimental pressure coefficient on the upper surface wit the computed results used in the present study. Transitio onset was determined by naphthalene flow visualizatio The experiments of Müller and Bippes[23] and Deyhle an Bippes[22] employed swept flat plates under the action favorable pressure gradients. The pressure coefficient me sured in the experiment is shown in Figure 9 for the thre tunnels used in the tests. Transition onset was determine by the location where $\Gamma = 0.5$

To facilitate comparisons with experiment, transitio onset was selected to be the point where $\Gamma = 0.5$. Thi assumes that the data reported in Radeztsky et al.[17] corre sponds to a location where $\Gamma = 0.5$. As noted from Fig. 1(which compares present theory with the data of Radezt sky et al.,[17] excellent agreement is noted for all Reynold numbers and surface finishes. For rms measured levels c

Table 3 Comparison of $Re_{x_c,tr}$ values at 50% intermittency predicted by the present method and measured in the swept plate experiments of Deyhle and Bippes.[22]

Facility	Tu	Plate Surface	Experimental $Re_{x,tr}$ (x10^5)	Present $Re_{x,tr}$ (x10^5)	Error (%)
NWB	0.08	Wooden plate, $\overline{R}_z = 6\mu m$	6.5	8.04	23.7
1MK	0.15	Plate with sandpaper. $\overline{R}_z = 40\mu m$	6.8	6.12	10.0
		Wooden plate,$\overline{R}_z = 6\mu m$	7.5	7.49	0.13
		Aluminum plate. sanded. $\overline{R}_z = 5\mu m$	7.7	7.63	0.9
		Aluminum plate. polished. $\overline{R}_z = 1.8\mu m$	8.3	8.48	2.17
1MK/screen	0.27	Aluminum plate. polished. $\overline{R}_z = 1.8\mu m$	7.8	7.11	8.85
NWG	0.57	Aluminum plate. sanded. $\overline{R}_z = 5\mu m$	5.4	2.18	59.6

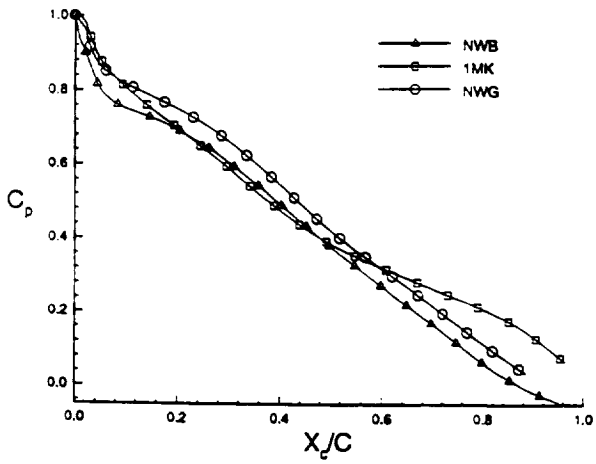

Figure 9 Experimental pressure coefficient along the swept plate of Deyhle and Bippes[22]

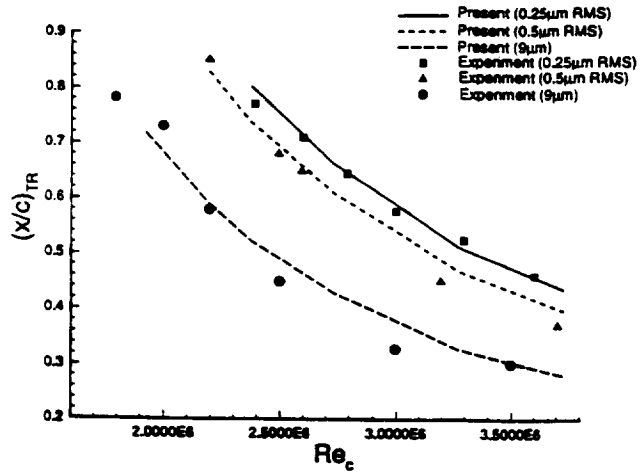

Figure 10 Comparison of the present method with the experimental data of Radestsky et al.[17]

surface roughness, a sinusoidal distribution is assumed and a "peak-to-peak" roughness level is established by multiplying the rms value by $\sqrt{2}$. The calculations assume a freestream intensity, $Tu = 0.09$, reported by Dagenhart.[25]

Table 3 compares present predictions with measurements reported by Deyhle and Bippes[22] using three different facilities and a variety of surface finishes. The 1MK tunnel is the $1 \times .07 m^2$ DLR facility in Göttingen, the NWB tunnel is the $3.25 \times 2.8 m^2$ DLR facility in Braunschweig, and the NWG tunnel is the $3 \times 3 m^2$ DLR facility in Göttingen. As may be seen from the table, excellent agreement is indicated for measurements taken in the 1MK facility. However, onset is overpredicted in the NWB tunnel and underpredicted in the NWG tunnel. The cause of the discrepancy in the NWB tunnel is not clear. On the other hand, the intensity in the NWG facility is high enough so that a by-pass mechanism may have been present.

CONCLUDING REMARKS

The present approach has developed, in the context of a CFD tool that employs turbulence modeling, a unified description for laminar, transitional, and turbulent flows. It allows for the presence of laminar fluctuations and treats them in a manner similar to that of turbulent flows. As a result, one can calculate the complete flowfield without having to use stability codes and at a cost comparable to that of existing CFD codes that employ two-equation turbulence models.

Although the e^n method or linear stability codes were not used in the calculations, results of stability theory played an important role in determining expressions for the eddy viscosity resulting from laminar fluctuations. Because the physics underlying T-S or CF instabilities are different, corresponding stress-strain laws governing the flowfield are different. Further work is needed to develop a stress-strain law that encompasses the effects of all relevant instabilities.

ACKNOWLEDGMENTS

This work is supported in part by NASA Grant NAG-1-1876. Part of the computations were carried out at the North Carolina Supercomputing Center and at the Numerical Aerospace Simulation (NAS) facilities.

The authors are indebted to a number of colleagues for providing relevant data and publications and for many helpful discussions. They are: Drs. Bill Saric of Arizona State University, Hans Bippes of DLR, Ray Dagenhart and Ron Joslin of NASA-Langley Research Center, and Nd Chokani from North Carolina State University.

REFERENCES

[1] Dhawan, S. and Narasimha, R., "Some Properties of Boundary Layer Flow During Transition from Lami-

nar to Turbulent Motion," *Journal of Fluid Mechanics*, Vol. 3, No. 4, 1958, pp. 418–436.

[2] Haynes, T.S., Reed, H.L., and Saric, W.S., "CFD Validation Issues in Transition Modeling," AIAA Paper 96–2057, June 1996.

[3] Young, T. W., Warren, E. S., Harris, J.E., and Hassan, H. A., "New Approach for the Calculation of Transitional Flows," *AIAA Journal*, Vol. 31, No. 4, April 1993, pp. 629–636.

[4] Warren, E. S., Harris, J. E., and Hassan, H. A., "A Transition Model for High-Speed Flow," *AIAA Journal*, Vol. 33, No. 8, August 1995, pp. 1391–1397.

[5] Warren, E.S., and Hassan, H.A. , "An Alternative to the e^n Method for Determining Onset of Transition," AIAA Paper 97–0825, January 1997.

[6] Warren, E.S., and Hassan, H.A. , "A Transition Model for Swept Wing Flows," AIAA Paper 97–2245, June 1997.

[7] Robinson, D. F., Harris, J. E., and Hassan, H. A., "Unified Turbulence Closure Model for Axisymmetric and Planar Free Shear Flows," *AIAA Journal*, Vol. 33, No. 12, December 1995, pp. 2325–2331.

[8] Wilcox, D. C., "Turbulence Model Transition Prediction," *AIAA Journal*, Vol. 13, No. 2, February 1975, pp. 241–243.

[9] Wilcox, D. C., "Alternative to the e^9 Procedure for Predicting Boundary-Layer Transition," *AIAA Journal*, Vol. 19, No. 1, January 1991, pp. 56–64.

[10] Wilcox, D. C., "The Remarkable Ability of Turbulence Model Equations to Describe Transition," *Fifth Symposium on Numerical and Physical Aspects of Aerodynamic Flows*, California State University, Long Beach, CA, January 1989.

[11] Chang, C.-L., Singer, B. A., Dinavahi, S. P. G., El-Hady, N. M., Harris, J. E., Streett, C. L., and Wilcox, D. C., "Transition Region Modeling for Compressible Flow," National Aerospace Plane CR 1142, February 1993.

[12] Wilcox, D. C., "Turbulence and Transition Modeling for High-Speed Flows," NASA Contractor Report 191473, April 1993.

[13] Robinson, D.F., and Hassan, H.A., "Modeling Turbulence Without Damping Functions Using $k - \zeta$ Model," AIAA Paper 97–2312, June 1997.

[14] Walker, G. J., "Transitional Flow on Axial Turbomachine Blading," *AIAA Journal*, Vol. 27, No. 5, May 1989, pp. 595–602.

[15] Schubauer, G.B., and Klebanoff, P.S., "Contributions on the Mechanics of Boundary-Layer Transition," NACA Report 1289, 1956.

[16] Schubauer, G.B., and Skramstad, H.K., "Laminar Boundary Layer Oscillations and Transition on a Flat Plate," NACA Report 909, 1948.

[17] Radeztsky, R.H. Jr., Reibert, M.S., Saric, W.S., and Takagi, S., "Effect of Micron-Sized Roughness on Transition in Swept-Wing Flows," AIAA Paper 93-0076, January 1993.

[18] Harris, J. E., and Blanchard, D. K., "Compute Program for Solving Laminar, Transitional, or Turbulent Compressible Boundary-Layer Equations for Two-Dimensional and Axisymmetric Flow," NASA TM 83207, February 1982.

[19] Gaffney, R.L., Jr., Salas, M.D., and Hassan, H.A. "An Abbreviated Reynolds Stress Turbulence Model for Airfoil Flows," AIAA Paper 90–1468, June 1990.

[20] Mateer, G. G., Monson, D. J., and Menter, F. R. "Skin-Friction Measurements and Calculations on a Lifting Airfoil," *AIAA Journal*, Vol. 34, No. 2, February 1996, pp. 231–236.

[21] Dagenhart, J.R., Saric, W.S., Hoos J.A., and Mousseux, M.C., "Experiments on Swept Wing Boundary Layers," *Laminar-Turbulent Transition IUTAM Symposium, Toulouse, France*, edited by D. Arnal and R. Michel, Springer Verlag, 1989.

[22] Deyhle, H., and Bippes, H., "Disturbance Growth in an Unstable Three-Dimensional Boundary Layer and its Dependence on Environmental Conditions," *Journal of Fluid Mechanics*, Vol. 316, June 1996, pp. 73-113.

[23] Müller, B., and Bippes, H., "Experimental Study of Instability Modes in a Three-Dimensional Boundary Layer," AGARD Report 438, October 1988.

[24] Schlichting, H., *Boundary-Layer Theory*, McGraw-Hill, seventh ed., 1979.

[25] Dagenhart, J., *Crossflow Stability and Transition experiments in a Swept-Wing Flow*, Ph.D. thesis, Virginia Polytechnic Institute and State University, 1992.